

## Establishment and cryptic transmission of Zika virus in Brazil and the Americas

Faria, N R; Quick, Joshua; Claro, I M; Thézé, J; de Jesus, J G; Giovanetti, M; Kraemer, M U G; Hill, S C; Black, A; da Costa, A C; Franco, L C; Silva, S P; Wu, C-H; Raghwani, J; Cauchemez, S; du Plessis, L; Verotti, M P; de Oliveira, W K; Carmo, E H; Coelho, G E

DOI:  
[10.1038/nature22401](https://doi.org/10.1038/nature22401)

License:  
None: All rights reserved

Document Version  
Peer reviewed version

### Citation for published version (Harvard):

Faria, NR, Quick, J, Claro, IM, Thézé, J, de Jesus, JG, Giovanetti, M, Kraemer, MUG, Hill, SC, Black, A, da Costa, AC, Franco, LC, Silva, SP, Wu, C-H, Raghwani, J, Cauchemez, S, du Plessis, L, Verotti, MP, de Oliveira, WK, Carmo, EH, Coelho, GE, Santelli, ACFS, Vinhal, LC, Henriques, CM, Simpson, JT, Loose, M, Andersen, KG, Grubaugh, ND, Somasekar, S, Chiu, CY, Muñoz-Medina, JE, Gonzalez-Bonilla, CR, Arias, CF, Lewis-Ximenez, LL, Baylis, SA, Chieppe, AO, Aguiar, SF, Fernandes, CA, Lemos, PS, Nascimento, BLS, Monteiro, HAO, Siqueira, IC, de Queiroz, MG, de Souza, TR, Bezerra, JF, Lemos, MR, Pereira, GF, Loudal, D, Moura, LC, Dhalia, R, França, RF, Magalhães, T, Marques, ET, Jaenisch, T, Wallau, GL, de Lima, MC, Nascimento, V, de Cerqueira, EM, de Lima, MM, Mascarenhas, DL, Neto, JPM, Levin, AS, Tozetto-Mendoza, TR, Fonseca, SN, Mendes-Correa, MC, Milagres, FP, Segurado, A, Holmes, EC, Rambaut, A, Bedford, T, Nunes, MRT, Sabino, EC, Alcantara, LCJ, Loman, NJ & Pybus, OG 2017, 'Establishment and cryptic transmission of Zika virus in Brazil and the Americas', *Nature*, vol. 546, no. 7658, pp. 406-410. <https://doi.org/10.1038/nature22401>

[Link to publication on Research at Birmingham portal](#)

**Publisher Rights Statement:**  
Checked for eligibility: 04/07/2017

### General rights

Unless a licence is specified above, all rights (including copyright and moral rights) in this document are retained by the authors and/or the copyright holders. The express permission of the copyright holder must be obtained for any use of this material other than for purposes permitted by law.

- Users may freely distribute the URL that is used to identify this publication.
- Users may download and/or print one copy of the publication from the University of Birmingham research portal for the purpose of private study or non-commercial research.
- User may use extracts from the document in line with the concept of 'fair dealing' under the Copyright, Designs and Patents Act 1988 (?)
- Users may not further distribute the material nor use it for the purposes of commercial gain.

Where a licence is displayed above, please note the terms and conditions of the licence govern your use of this document.

When citing, please reference the published version.

### Take down policy

While the University of Birmingham exercises care and attention in making items available there are rare occasions when an item has been uploaded in error or has been deemed to be commercially or otherwise sensitive.

If you believe that this is the case for this document, please contact [UBIRA@lists.bham.ac.uk](mailto:UBIRA@lists.bham.ac.uk) providing details and we will remove access to the work immediately and investigate.

Download date: 04. May. 2023

1 **Establishment and cryptic transmission of Zika virus in Brazil and the Americas**

2

3 Faria, N. R.<sup>\*1,2</sup>, Quick, J.<sup>3\*</sup>, Morales, I.<sup>4\*</sup>, Thézé, J.<sup>1\*</sup>, Jesus, J.G.<sup>5\*</sup>, Giovanetti,  
4 M.<sup>5,6\*</sup>, Kraemer, M. U. G.<sup>1,7,8\*</sup>, Hill, S. C.<sup>1\*</sup>, Black, A.<sup>9,10\*</sup>, da Costa, A. C.<sup>4</sup>, Franco,  
5 L.C.<sup>2</sup>, Silva, S. P.<sup>2</sup>, Wu, C.-H.<sup>11</sup>, Raghwani, J.<sup>1</sup>, Cauchemez, S.<sup>12,13</sup>, du Plessis, L.<sup>1</sup>,  
6 Verotti, M. P.<sup>14</sup>, de Oliveira, W. K.<sup>15,16</sup>, Carmo, E. H.<sup>17</sup>, Coelho, G. E.<sup>18,19</sup>, Santelli, A.  
7 C. F. S.<sup>18,20</sup>, Vinhal, L. C.<sup>18</sup>, Henriques, C. M.<sup>17</sup>, Simpson, J. T.<sup>21</sup>, Loose, M.<sup>22</sup>,  
8 Andersen, K. G.<sup>23</sup>, Grubaugh, N. D.<sup>23</sup>, Somasekar, S.<sup>24</sup>, Chiu, C. Y.<sup>24</sup>, Muñoz-  
9 Medina, J. E.<sup>25</sup>, Gonzalez-Bonilla, C. R.<sup>25</sup>, Arias, C. F.<sup>26</sup>, Lewis-Ximenez, L. L.<sup>27</sup>,  
10 Baylis, S.A.<sup>28</sup>, Chieppe, A. O.<sup>29</sup>, Aguiar, S. F.<sup>29</sup>, Fernandes, C. A.<sup>29</sup>, Lemos, P. S.<sup>2</sup>,  
11 Nascimento, B. L. S.<sup>2</sup>, Monteiro, H. A. O.<sup>2</sup>, Siqueira, I. C.<sup>5</sup>, de Queiroz, M. G.<sup>30</sup>, de  
12 Souza, T. R.<sup>30,31</sup>, Bezerra, J. F.<sup>30,32</sup>, Lemos, M. R.<sup>33</sup>, Pereira, G. F.<sup>33</sup>, Loudal, D.<sup>33</sup>,  
13 Moura, L. C.<sup>33</sup>, Dhalia, R.<sup>34</sup>, França, R. F.<sup>34</sup>, Magalhães, T.<sup>34</sup>, Marques, E. T. Jr.<sup>34,35</sup>,  
14 Jaenisch, T.<sup>36</sup>, Wallau, G. L.<sup>34</sup>, de Lima, M. C.<sup>37</sup>, Nascimento, V.<sup>37</sup>, de Cerqueira, E.  
15 M.<sup>38</sup>, de Lima, M. M.<sup>38</sup>, Mascarenhas, D. L.<sup>39</sup>, Moura Neto, J. P.<sup>40</sup>, Levin, A. S.<sup>4</sup>,  
16 Tozetto-Mendoza, T. R.<sup>4</sup>, Fonseca, S. N.<sup>41</sup>, Mendes-Correa, M. C.<sup>4</sup>, Milagres, F.P.<sup>42</sup>,  
17 Segurado, A.<sup>4</sup>, Holmes, E. C.<sup>43</sup>, Rambaut, A.<sup>44,45</sup>, Bedford, T.<sup>9</sup>, Nunes, M. R. T.<sup>\*2,46</sup>,  
18 Sabino, E. C.<sup>47\*</sup>, Alcantara, L. C. J.<sup>51\*</sup>, Loman, N.<sup>31\*</sup>, Pybus, O. G.<sup>1,47\*</sup>

19

20

21 **Affiliations:**

- 22 1. Department of Zoology, University of Oxford, Oxford OX3 1PS, UK  
23 2. Evandro Chagas Institute, Ministry of Health, Ananindeua, Brazil  
24 3. Institute of Microbiology and Infection, University of Birmingham, UK  
25 4. Department of Infectious Disease, School of Medicine & Institute of Tropical  
26 Medicine, University of São Paulo, Brazil  
27 5. Fundação Oswaldo Cruz (FIOCRUZ), Salvador, Bahia, Brazil  
28 6. University of Rome Tor Vergata, Rome, Italy  
29 7. Harvard Medical School, Boston, MA, USA  
30 8. Boston Children's Hospital, Boston, MA, USA  
31 9. Vaccine and Infectious Disease Division, Fred Hutchinson Cancer Research  
32 Center, Seattle, WA, USA  
33 10. Department of Epidemiology, University of Washington, Seattle, WA, USA  
34 11. Department of Statistics, University of Oxford, Oxford OX3 1PS, UK  
35 12. Mathematical Modelling of Infectious Diseases and Center of Bioinformatics,  
36 Biostatistics and Integrative Biology, Institut Pasteur, Paris, France  
37 13. Centre National de la Recherche Scientifique, URA3012, Paris, France  
38 14. Coordenação dos Laboratórios de Saúde (CGLAB/DEVIT/SVS), Ministry of  
39 Health, Brasília, Brazil  
40 15. Coordenação Geral de Vigilância e Resposta às Emergências em Saúde Pública  
41 (CGVR/DEVIT), Ministry of Health, Brasília, Brazil  
42 16. Center of Data and Knowledge Integration for Health (CIDACS), Fundação  
43 Oswaldo Cruz (FIOCRUZ), Brazil  
44 17. Departamento de Vigilância das Doenças Transmissíveis, Ministry of Health,  
45 Brasília, Brazil  
46 18. Coordenação Geral dos Programas de Controle e Prevenção da Malária e das  
47 Doenças Transmitidas pelo *Aedes*, Ministry of Health, Brasília, Brazil  
48 19. Pan American Health Organization (PAHO), Buenos Aires, Argentina  
49 20. Fundação Oswaldo Cruz (FIOCRUZ), Rio de Janeiro, Brazil

21. Ontario Institute for Cancer Research, Toronto, Canada
22. University of Nottingham, Nottingham, UK
23. Department of Immunology and Microbial Science, The Scripps Research Institute, La Jolla, CA 92037, USA
24. Departments of Laboratory Medicine and Medicine & Infectious Diseases, University of California, San Francisco, USA
25. División de Laboratorios de Vigilancia e Investigación Epidemiológica, Instituto Mexicano del Seguro Social, Ciudad de México, Mexico
26. Instituto de Biotecnología, Universidad Nacional Autónoma de México, Cuernavaca, Mexico
27. Instituto Oswaldo Cruz (FIOCRUZ), Rio de Janeiro, Brazil
28. Paul-Ehrlich-Institut, Langen, Germany
29. Laboratório Central de Saúde Pública Noel Nutels, Rio de Janeiro, Brazil
30. Laboratório Central de Saúde Pública do Estado do Rio Grande do Norte, Natal, Brazil
31. Universidade Potiguar do Rio Grande do Norte, Natal, Brazil
32. Faculdade Natalense de Ensino e Cultura, Rio Grande do Norte, Natal, Brazil
33. Laboratório Central de Saúde Pública do Estado da Paraíba, João Pessoa, Brazil
34. Fundação Oswaldo Cruz (FIOCRUZ), Recife, Pernambuco, Brazil
35. Center for Vaccine Research, Graduate School of Public Health, University of Pittsburgh, Pittsburgh, PA, USA
36. Section Clinical Tropical Medicine, Department for Infectious Diseases, Heidelberg University Hospital, Heidelberg, Germany
37. Laboratório Central de Saúde Pública do Estado de Alagoas, Maceió, Brazil
38. Universidade Estadual de Feira de Santana, Feira de Santana, Bahia, Brazil
39. Secretaria de Saúde de Feira de Santana, Feira de Santana, Bahia, Brazil
40. Universidade Federal do Amazonas, Manaus, Brazil
41. Hospital São Francisco, Ribeirão Preto, Brazil
42. Universidade Federal do Tocantins, Palmas, Brazil
43. University of Sydney, Sydney, Australia
44. Institute of Evolutionary Biology, University of Edinburgh, Edinburgh EH9 3FL, UK
45. Fogarty International Center, National Institutes of Health, Bethesda, MD 20892, USA
46. Department of Pathology, University of Texas Medical Branch, Galveston, TX 77555, USA
47. Metabiota, San Francisco, CA 94104, USA

**\* Joint first or senior author**

**One Sentence Summary:** Virus genomes reveal the establishment of Zika virus in Brazil and the Americas, and provide an appropriate timeframe for baseline (pre-Zika) microcephaly in different regions.

Transmission of Zika virus (ZIKV) in the Americas was first confirmed in May 2015 in northeast Brazil<sup>1</sup>. Brazil has had the highest number of reported ZIKV cases worldwide (more than 200,000 by 24 December 2016<sup>2</sup>) and the most cases associated with microcephaly and other birth defects (2,366 confirmed by 31 December 2016<sup>2</sup>). Since the initial detection of ZIKV in Brazil, more than 45 countries in the Americas have reported local ZIKV transmission, with 24 of these reporting severe ZIKV-associated disease<sup>3</sup>. However, the origin and epidemic history of ZIKV in Brazil and the Americas remain poorly understood, despite the value of this information for interpreting observed trends in reported microcephaly. Here we address this issue by generating 54 complete or partial ZIKV genomes, mostly from Brazil, and reporting data generated by a mobile genomics laboratory that travelled across northeast Brazil in 2016. One sequence represents the earliest confirmed ZIKV infection in Brazil. Analyses of viral genomes with ecological and epidemiological data yield an estimate that ZIKV was present in northeast Brazil by February 2014 and is likely to have disseminated from there, nationally and internationally, before the first detection of ZIKV in the Americas. Estimated dates for the international spread of ZIKV from Brazil indicate the duration of pre-detection cryptic transmission in recipient regions. The role of northeast Brazil in the establishment of ZIKV in the Americas is further supported by geographic analysis of ZIKV transmission potential and by estimates of the basic reproduction number of the virus.

Previous phylogenetic analyses have indicated that the ZIKV epidemic was caused by the introduction of an Asian genotype lineage into the Americas around late 2013, at least one year before its detection there<sup>4</sup>. An estimated 100 million people in the Americas are predicted to be at risk of acquiring ZIKV once the epidemic has reached its full extent<sup>5</sup>. However, little is known about the genetic diversity and transmission history of the virus in Brazil<sup>6</sup>. Reconstructing the spread of ZIKV from case reports alone is challenging because symptoms (typically fever, headache, joint pain, rashes, and conjunctivitis) overlap with those caused by co-circulating arthropod-borne viruses<sup>7</sup> and owing to a lack of nationwide ZIKV-specific surveillance in Brazil before 2016.

We undertook a collaborative investigation of the molecular epidemiology of ZIKV in Brazil, including results from a mobile genomics laboratory that travelled through northeast Brazil during June 2016 (the ZiBRA project; <http://www.zibraproject.org>). Of five regions of Brazil (**Fig. 1a**), the northeast region has the most notified ZIKV cases (40% of Brazilian cases) and the most confirmed microcephaly cases (76% of Brazilian cases, as of 31 December 2016<sup>2</sup>), raising questions about why the region has been so severely affected<sup>8</sup>. Furthermore, northeast Brazil is the most populous region of Brazil that also has potential for year-round ZIKV transmission<sup>9</sup>. With support from the Brazilian Ministry of Health and other institutions (see **Acknowledgements**), the ZiBRA laboratory screened 1,330 samples (almost exclusively serum or blood) from patients in 82 municipalities across 5 federal states (**Fig. 1, Extended Data Table 1a**). Samples provided by the public health laboratories of each state (LACEN) and the Fundação Oswaldo Cruz (FIOCRUZ) were screened for the presence of ZIKV by real-time quantitative PCR (RT-qPCR).

On average, ZIKV viraemia persists for 10 days after infection; symptoms develop after about 6 days and can last for 1–2 weeks<sup>10</sup>. In line with previous



147 observations in Colombia<sup>11</sup>, we found that RT-qPCR-positive samples from northeast  
 148 Brazil were, on average, collected only 2 days after the onset of symptoms. The  
 149 median RT-qPCR cycle threshold (Ct) value of positive samples was correspondingly  
 150 high, at 36 (**Extended Data Fig. 1a, b**). For northeast Brazil, the time series of RT-  
 151 qPCR+ cases was positively correlated with the number of weekly notified cases  
 152 (Pearson's  $\rho = 0.62$ ; **Fig. 1b**).

153 The ability of the mosquito vector *Aedes aegypti* to transmit ZIKV is  
 154 determined by ecological factors that affect adult survival, viral replication, and  
 155 infective periods<sup>12</sup>. To investigate the receptivity of Brazilian regions to ZIKV  
 156 transmission we used a measure of vector climatic suitability, derived from monthly  
 157 temperature, relative humidity, and precipitation data<sup>13</sup>. Using linear regression we  
 158 noted that, for each Brazilian region, there is a strong association between estimated  
 159 climatic suitability and weekly notified cases (**Fig. 1b, c**; adjusted  $R^2 > 0.84$ ,  $P <$   
 160  $0.001$ ; **Extended Data Table 1b**). Similar to previous findings from dengue virus  
 161 outbreaks<sup>14,15</sup>, notified ZIKV cases lag climatic suitability by about 4–6 weeks in all  
 162 regions, except northeast Brazil, where no time lag is evident. Despite these  
 163 associations, numbers of notified cases should be interpreted cautiously because co-  
 164 circulating dengue and chikungunya viruses exhibit symptoms similar to ZIKV, and  
 165 the Brazilian case reporting system has evolved through time (see **Methods**). We  
 166 estimated basic reproductive numbers ( $R_0$ ) for ZIKV in each Brazilian region from the  
 167 weekly notified case data and found that  $R_0$  was high in northeast Brazil ( $R_0$  around 3  
 168 for both epidemic seasons; **Extended Data Table 1c**). Although our  $R_0$  values are  
 169 approximate, in part owing to spatial variation in transmission across the large regions  
 170 analysed here, they are consistent with estimates from other approaches<sup>16,17</sup>.

171 Encouraged by the utility of portable genomic technologies during the West  
 172 African Ebola virus epidemic<sup>18</sup> we used our open protocol<sup>19</sup> to sequence ZIKV  
 173 genomes directly from clinical material using MinION DNA sequencers. We were  
 174 able to generate virus sequences within 48h of the mobile laboratory's arrival at each  
 175 LACEN. In pilot experiments using a cultured ZIKV reference strain<sup>20</sup> we recovered  
 176 98% of the virus genome (**Extended Data Fig. 1c**). However, owing to low viral  
 177 copy numbers in clinical samples (**Extended Data Fig. 1a**), many sequences  
 178 exhibited incomplete genome coverage and required additional sequencing efforts in  
 179 static labs once fieldwork had been completed. Whereas average genome coverage  
 180 was typically high for samples with lower Ct values (85% for  $Ct < 33$ ; **Fig. 2a**,  
 181 **Extended Data Table 2**), samples with higher Ct values had variable coverage (mean  
 182 72% for  $Ct > 33$ ; **Fig. 2a**). Unsequenced genome regions were non-randomly  
 183 distributed (**Fig. 2b**), suggesting that the efficiency of PCR amplification varied  
 184 among primer pair combinations. We generated 36 near-complete or partial genomes  
 185 from the northeast, southeast and northern regions of Brazil, supplemented by nine  
 186 sequences from samples from Rio de Janeiro municipality. To further reconstruct Zika  
 187 virus transmission in the Americas, we include five new complete ZIKV genomes  
 188 from Colombia and four from Mexico. In addition, we append to our dataset 115  
 189 publicly available sequences and 85 additional genomes from ref. 21. The final  
 190 dataset comprised 254 ZIKV sequences, 241 of which were sampled in the Americas  
 191 (see **Methods**).

192 The American ZIKV epidemic comprises a single founder lineage<sup>4,22,23</sup>  
 193 (hereafter termed Am-ZIKV) derived from Asian genotype viruses (hereafter termed  
 194 PreAm-ZIKV) from southeast Asia and the Pacific<sup>4</sup>. A sliding window analysis of  
 195 pairwise genetic diversity along the ZIKV genome shows that the diversity of PreAm-  
 196 ZIKV strains is on average about two-fold greater than that of Am-ZIKV viruses (**Fig.**

197 **2d**), reflecting a longer period of ZIKV circulation in Asia and the Pacific than in the  
198 Americas. The genetic diversity of Am-ZIKV strains will increase in the future and  
199 updated diagnostic assays are recommended to guarantee RT-qPCR sensitivity<sup>24</sup>.

200 It has been suggested that recent ZIKV epidemics may be linked causally to a  
201 higher apparent evolutionary rate for the Asian genotype than the African  
202 genotype<sup>25,26</sup>. However, such comparisons are confounded by an inverse relationship  
203 between the timescale of observation and estimated evolutionary rates<sup>27</sup>. Regression  
204 of sequence sampling dates against root-to-tip genetic distances indicates that  
205 molecular clock models can be applied reliably to the Asian ZIKV lineage (**Fig. 2c**,  
206 **Extended Data Figs 2, 3**). We estimate the whole-genome evolutionary rate of Asian  
207 ZIKV to be  $1.12 \times 10^{-3}$  substitutions per site per year (95% Bayesian credible interval  
208 (BCI)  $0.97\text{--}1.27 \times 10^{-3}$ ), consistent with other estimates for this lineage<sup>4,26</sup>. We found  
209 no significant differences in evolutionary rates among ZIKV genome regions  
210 (**Extended Data Table 3a**). The estimated ratio of divergence at nonsynonymous and  
211 synonymous sites (dN/dS) of the Am-ZIKV lineage is low (0.11, 95% confidence  
212 interval 0.10–0.13), as observed for other vector-borne flaviviruses<sup>28</sup>, but is higher  
213 than that of PreAm-ZIKV viruses (0.061, 0.047–0.077), probably owing to the raised  
214 probability of observing slightly deleterious changes in short-term datasets, as  
215 observed during previous epidemics<sup>29</sup>.

216 We used two phylogeographic approaches with different assumptions<sup>30,31</sup> to  
217 reconstruct the origins and spread of ZIKV in Brazil and the Americas. We dated the  
218 common ancestor of ZIKV in the Americas (node B, **Fig. 3**) to Jan 2014 (95% BCI  
219 October 2013–April 2014; **Extended Data Tables 3b, c**), in line with previous  
220 estimates<sup>4,26</sup>. We find evidence that northeast Brazil played a central role in the  
221 establishment and dissemination of Am-ZIKV. Although northeast Brazil is the most  
222 probable location of node B (location posterior support 0.83, **Fig. 3**), the current data  
223 do not allow us to exclude the hypothesis that node B was in the Caribbean (**Fig. 3**  
224 dashed branches) owing to the presence of two sequences from Haiti in one of its  
225 descendant lineages. More importantly, most Am-ZIKV sequences descend from a  
226 radiation of lineages (node C and its immediate descendants; **Fig. 3**) dated to late  
227 February 2014 (95% BCIs of node C, November 2013–May 2014). Node C is more  
228 strongly inferred to have existed in northeast Brazil (location posterior support 0.99,  
229 **Fig. 3**). All 20 replicate analyses performed on subsampled datasets place node C in  
230 Brazil, and 14 of them place node C in northeast Brazil (**Extended Data Fig. 4**).  
231 Consequently, we conclude that node C reflects the crucial turning point in the  
232 emergence of ZIKV in the Americas. If further data show that node B did exist in  
233 Haiti, then it is likely that Haiti acted as an intermediate ‘stepping stone’ for the  
234 arrival and establishment of Am-ZIKV in Brazil, from where the virus subsequently  
235 spread to other regions. This perspective is consistent with the lower population size  
236 of Haiti compared to Brazil. We infer that node C was present in northeast Brazil  
237 several months before three notable events, each of which also occurred in northeast  
238 Brazil: (i) the retrospective identification of a cluster of suspected but unconfirmed  
239 ZIKV cases in December 2014<sup>1</sup>; (ii) the collection of the oldest ZIKV genome  
240 sequence from Brazil, reported here, sampled in February 2015; and (iii) confirmation  
241 of cases of ZIKV transmission in northeast Brazil in March 2015<sup>32,33</sup>.

242 Our results further indicate that viruses from northeast Brazil were important  
243 for the continental spread of ZIKV. Within Brazil, we find instances of virus lineage  
244 movement from northeast to southeast Brazil; most of these events are dated to the  
245 second half of 2014 and led to onwards transmission in Rio de Janeiro (RJ1–RJ4; **Fig.**  
246 **3**) and São Paulo states (SP1; **Fig. 3**). We infer that ZIKV lineages disseminated from

northeast Brazil to elsewhere in Central America, the Caribbean, and South America. Most Am-ZIKV strains sampled outside Brazil fall into four well-supported phylogenetic groups (**Fig. 3**); three (SA1/CB1, CA1 and SA2) are inferred to have been exported from northeast Brazil between July 2014 and April 2015, whereas the Caribbean clade CB2 appears to have originated from southeast Brazil around March 2015 (**Figs 3, 4**). Each viral lineage export occurred during a period of climatic suitability for vector transmission in the recipient location (**Fig. 4**). For the earliest exports to Central America (CA1) and South America (SA1), there is an estimated 11–12-month gap between the date of export and the date of ZIKV detection in the recipient location, suggesting a complete season of undetected transmission. These periods of cryptic transmission are relevant to studies of spatiotemporal trends in reported microcephaly, because they help to define the appropriate timeframe for baseline (pre-ZIKV) microcephaly in each region.

Large-scale surveillance of ZIKV is challenging because many cases may be asymptomatic, and ZIKV co-circulates in some regions with other arthropod-borne viruses that have overlapping symptoms (for example, dengue, chikungunya, Mayaro, and Oropouche viruses). However combining virus genomic and epidemiological data can generate insights into vector-borne virus transmission. A system of continuous and structured virus sequencing in Brazil, integrated with surveillance data, could provide timely information to inform effective responses against Zika and other viruses, including the recently re-emerged yellow fever virus<sup>34</sup>.

## References

- 1 Kindhauser, M. K., Allen, T., Frank, V., Santhana, R. S. & Dye, C. Zika: the origin and spread of a mosquito-borne virus. *Bulletin of the World Health Organization* **94**, 675-686C, doi:10.2471/BLT.16.171082 (2016).
- 2 Ministério da Saúde. Boletins Epidemiológicos—Secretaria de Vigilância em Saúde <http://portalsaude.saude.gov.br/index.php/o-ministerio/principal/secretarias/svs/boletim-epidemiologico> (2017).
- 3 WHO. Situation Report - Zika virus, microcephaly, Guillain-Brarré syndrome (18 Jan 2017). (<http://apps.who.int/iris/bitstream/10665/253604/1/zikasitrep20Jan17-eng.pdf?ua=1>, 2017).
- 4 Faria, N. R. *et al.* Zika virus in the Americas: Early epidemiological and genetic findings. *Science* **352**, 345-349, doi:10.1126/science.aaf5036 (2016).
- 5 Alex Perkins, T., Siraj, A. S., Ruktanonchai, C. W., Kraemer, M. U. & Tatem, A. J. Model-based projections of Zika virus infections in childbearing women in the Americas. *Nat Microbiol* **1**, 16126, doi:10.1038/nmicrobiol.2016.126 (2016).
- 6 Lessler, J. *et al.* Assessing the global threat from Zika virus. *Science* **353**, aaf8160, doi:10.1126/science.aaf8160 (2016).
- 7 Vasconcelos, P. F. & Calisher, C. H. Emergence of Human Arboviral Diseases in the Americas, 2000-2016. *Vector Borne and Zoonotic Diseases* **16**, 295-301, doi:10.1089/vbz.2016.1952 (2016).
- 8 Vogel, G. One year later, Zika scientists prepare for a long war. *Science* **354**, 1088-1089 (2016).
- 9 Bogoch, II *et al.* Potential for Zika virus introduction and transmission in resource-limited countries in Africa and the Asia-Pacific region: a modelling

study. *The Lancet Infectious Diseases* **16**, 1237-1245, doi:10.1016/S1473-3099(16)30270-5 (2016).

10 Lessler, J. T., Ott, C.T., Carcelen, A.C., Konikoff, J.M., Williamson, J., Bi, Q., et al. . Times to key events in the course of Zika infection and their implications: a systematic review and pooled analysis [Submitted]. *Bull World Health Organ* DOI: **10.2471/BLT.16.174540** (2016).

11 Pacheco, O. *et al.* Zika Virus Disease in Colombia - Preliminary Report. *The New England Journal of Medicine*, doi:10.1056/NEJMoa1604037 (2016).

12 Liu-Helmersson, J., Stenlund, H., Wilder-Smith, A. & Rocklov, J. Vectorial capacity of *Aedes aegypti*: effects of temperature and implications for global dengue epidemic potential. *PloS One* **9**, e89783, doi:10.1371/journal.pone.0089783 (2014).

13 Cuong, H. Q. *et al.* Quantifying the emergence of dengue in Hanoi, Vietnam: 1998-2009. *PLoS Negl Trop Dis* **5**, e1322, doi:10.1371/journal.pntd.0001322 (2011).

14 Gharbi, M. *et al.* Time series analysis of dengue incidence in Guadeloupe, French West Indies: forecasting models using climate variables as predictors. *BMC Infectious Diseases* **11**, 166, doi:10.1186/1471-2334-11-166 (2011).

15 Caminade, C. *et al.* Global risk model for vector-borne transmission of Zika virus reveals the role of El Nino 2015. *PNAS* **114**, 119-124, doi:10.1073/pnas.1614303114 (2017).

16 Rocklov, J. *et al.* Assessing Seasonal Risks for the Introduction and Mosquito-borne Spread of Zika Virus in Europe. *EBioMedicine* **9**, 250-256, doi:10.1016/j.ebiom.2016.06.009 (2016).

17 Quick, J. *et al.* Real-time, portable genome sequencing for Ebola surveillance. *Nature* **530**, 228-232, doi:10.1038/nature16996 (2016).

18 Quick J., *et al.* Multiplex PCR method for MinION and Illumina sequencing of Zika and other virus genomes directly from clinical samples. *Nature Protocols* in press (2017).

19 Trosmeier, J. H. *et al.* Genome Sequence of a Candidate World Health Organization Reference Strain of Zika Virus for Nucleic Acid Testing. *Genome Announcements* **4**, doi:10.1128/genomeA.00917-16 (2016).

20 Metsky, H. C. *et al.* Genome sequencing reveals Zika virus diversity and spread in the Americas. *bioRxiv* <https://doi.org/10.1101/109348> (2017).

21 Giovanetti, M. *et al.* Zika virus complete genome from Salvador, Bahia, Brazil. *Infection, Genetics and Evolution* **41**, 142-145, doi:10.1016/j.meegid.2016.03.030 (2016).

22 Naccache, S. N. *et al.* Distinct Zika Virus Lineage in Salvador, Bahia, Brazil. *Emerging Infectious Diseases* **22**, doi:10.3201/eid2210.160663 (2016).

23 Corman, V. M. *et al.* Assay optimization for molecular detection of Zika virus. *Bulletin of the World Health Organization* **94**, 880-892, doi:10.2471/BLT.16.175950 (2016).

24 Liu, H. *et al.* From discovery to outbreak: the genetic evolution of the emerging Zika virus. *Emerg Microbes Infect* **5**, e111, doi:10.1038/emi.2016.109 (2016).

25 Pettersson, J. H. O., Eldholm, V., Seligmna, S. J., Lundkvist, A., Falconar, A. K., Gaunt, M. W., Musso, D., Nougairede, A., Charrel, R., Gould, E. A., Lamballerie, X. How Did Zika Virus Emerge in the Pacific Islands and Latin America? *mBio* **7**, 201239-201216 (2016).

- 26 Holmes, E. C., Dudas, G., Rambaut, A. & Andersen, K. G. The evolution of Ebola virus: Insights from the 2013-2016 epidemic. *Nature* **538**, 193-200, doi:10.1038/nature19790 (2016).
- 27 Holmes, E. C. Patterns of intra- and interhost nonsynonymous variation reveal strong purifying selection in dengue virus. *Journal of Virology* **77**, 11296-11298 (2003).
- 28 Park, D. J. *et al.* Ebola Virus Epidemiology, Transmission, and Evolution during Seven Months in Sierra Leone. *Cell* **161**, 1516-1526, doi:10.1016/j.cell.2015.06.007 (2015).
- 29 De Maio, N., Wu, C. H., O'Reilly, K. M. & Wilson, D. New Routes to Phylogeography: A Bayesian Structured Coalescent Approximation. *PLoS Genetics* **11**, e1005421, doi:10.1371/journal.pgen.1005421 (2015).
- 30 Lemey, P., Rambaut, A., Drummond, A. J. & Suchard, M. A. Bayesian phylogeography finds its roots. *PLoS Computational Biology* **5**, e1000520, doi:10.1371/journal.pcbi.1000520 (2009).
- 31 Campos, G. S., Bandeira, A. C. & Sardi, S. I. Zika Virus Outbreak, Bahia, Brazil. *Emerging Infectious Diseases* **21**, 1885-1886, doi:10.3201/eid2110.150847 (2015).
- 32 Zanicola, C. *et al.* First report of autochthonous transmission of Zika virus in Brazil. *Memorias do Instituto Oswaldo Cruz* **110**, 569-572, doi:10.1590/0074-02760150192 (2015).
- 33 Paules, C. I., Fauci, A. S. Yellow Fever — Once Again on the Radar Screen in the Americas. *The New England Journal of Medicine* (2017).

**Supplementary Information** is available in the online version of the paper.

**Acknowledgments:** We are deeply grateful to Fundação Oswaldo Cruz in Bahia and Pernambuco states, University of São Paulo, Instituto Evandro Chagas, and the Brazilian Zika virus surveillance network for their essential contributions. We thank the following for giving us permission to use their unpublished genomes available on GenBank: Robert Lanciotti (CDC, USA), John Lednicky (University of Florida, USA), Antoine Enfissi (Institut Pasteur de la Guyane), F. Baldanti (Pavia University, Italy), Reed Shabman (ATCC, USA), Brett Pickett (JCVI, USA), Raymond Schinazi (Emory University, USA), Myrna Bonaldo (Instituto Oswaldo Cruz, Rio de Janeiro, Brazil), Michael Gale (University of Washington, USA), Maria Capobianchi and Catilietti Concetta (INMI "L. Spallanzani", Italy), Mariana Leguia (NAMRU6, Peru), José Alberto Diaz (InDRE, Mexico), Edgar Sevilla-Reyes (INER, Mexico), Alexander Franz (University of Missouri, USA), Mariano Garcia-Blanco (Duke University, USA), MJ van Hemert (LUMC, Netherlands). We thank Pedro Fernando da Costa Vasconcelos, Sueli Guerreiro Rodrigues, Jedson Cardoso, Janaina Vasconcelos, João Vianez Junior (Instituto Evandro Chagas, Brazil), Juliana Gil Melgaço (FIOCRUZ, Rio de Janeiro, Brazil), Johannes Blumel (Paul-Ehrlich-Institut, Langen, Germany), Marcia Cristina Brito Lobato, Liliana Nunes Fava (Tocantins State Department of Health, Brazil), Constância Ayres (Instituto Aggeu Magalhães, Brazil) and Filipa Campos. LCJA thanks QIAGEN for reagents and equipment, MRTN thanks FERPEL for consumables. We thank Oxford Nanopore for technical support, particularly Rosemary Dokos, Zoe McDougall, Simon Cowan, Gordon Sanghera, and Oliver Hartwell. This work was supported by a MRC/Wellcome Trust/Newton Fund Zika Rapid Response grant (MC\_PC\_15100/ZK/16-078) and by the USAID Emerging Pandemic Threats Program-2 PREDICT-2 (Cooperative

394 Agreement AID-OAA-A-14-00102). NJL is supported by a MRC Bioinformatics  
 395 Fellowship. NRF is funded by a Sir Henry Dale Fellowship (grant 204311/Z/16/Z).  
 396 CNPq contributed to trip expenses (grant 457480/2014-9). ACC was supported by  
 397 FAPESP #2012/03417-7 and MRTN by CNPq grant no. 302584/2015-3. AB and TB  
 398 were supported by NIH award R35 GM119774. AB is supported by NSF Graduate  
 399 Research Fellowship Program (grant DGE-1256082). TB is a Pew Biomedical  
 400 Scholar. CYC is partially supported by NIH grant R01 HL105704 and an award from  
 401 Abbott Laboratories, Inc. EH is supported by a National Health and Medical Research  
 402 Council Australia Fellowship (GNT1037231). C.-H.W. is supported by MRC and  
 403 CRUK (ANR00310) and by Wellcome Trust and Royal Society (grant  
 404 101237/Z/13/Z). SCH is supported by the Wellcome Trust. This research received  
 405 funding from the ERC under grant agreements 614725-PATHPHYLODYN and  
 406 278433-PREDEMICS, and from EU Horizon 2020 under agreements 643476-  
 407 COMPARE and 734548-ZIKAlliance. TJ and ETJM acknowledge funding from  
 408 IDAMS, DENFREE, DengueTools, and PPSUS-FACEPE (project APQ-0302-  
 409 4.01/13). RFF received funding from FACEPE (APQ-0044.2.11/16 and APQ-  
 410 0055.2.11/16) and from CNPq (439975/2016-6). SAB was supported by the  
 411 Sicherheit von Blut und Geweben hinsichtlich der Abwesenheit von Zikaviren from  
 412 the German Ministry of Health.

413  
 414 **Author Contributions:** NRF, LCJA, MRTN, ECS, NL and OGP designed the study.  
 415 NRF, JQ, NL, IM, JGJ, MG, SCH, AB, ACdC, LCF, SPS, TB, PSL, BLN, HAOM,  
 416 MRTN, and LCJA undertook fieldwork and experiments. NRF, JT, C-HW, OGP, JR  
 417 and LdP performed genetic analyses. NRF, MUG, OGP and SC performed  
 418 epidemiological analyses. NRF, JQ, MUGK, NL and OGP wrote the manuscript.  
 419 ECH, AR, TB, MRTN, ECS and LCJA edited the manuscript. Other authors were  
 420 critical for coordination, collection, processing, sequencing and bioinformatics of  
 421 samples. All authors read and approved the contents of the manuscript.

422  
 423 **Competing Financial Interests:** NJL received speaking fees from Oxford Nanopore  
 424 Technologies (ONT) and has received free-of-charge reagents in support of the  
 425 ZiBRA project from ONT. OGP receives consultancy income from Metabiota Inc,  
 426 CA, USA. CYC is the director of the UCSF-Abbott Viral Diagnostics and Discovery  
 427 Center and receives research support from Abbott Laboratories, Inc.

428  
 429 **Author Information:** Reprints and permissions information is available at  
 430 [www.nature.com/reprints](http://www.nature.com/reprints). Correspondence and requests for materials should be  
 431 addressed to L.C.J.A. ([lalcan@bahia.fiocruz.br](mailto:lalcan@bahia.fiocruz.br)), E.C.S. ([sabinoec@usp.br](mailto:sabinoec@usp.br)), N.J.L.  
 432 ([n.j.loman@bham.ac.uk](mailto:n.j.loman@bham.ac.uk)), and O.G.P. ([oliver.pybus@zoo.ox.ac.uk](mailto:oliver.pybus@zoo.ox.ac.uk)).  
 433  
 434

**Fig. 1. Geographic and temporal distribution of ZIKV in Brazil.** **a.** Sampling location of genome sequences from Brazil and the Americas. Federal states in Brazil are coloured according to 5 geographic regions (lower inset). A red line surrounds the states surveyed by the ZiBRA mobile lab in 2016. State codes are PA=Pará, MA=Maranhão, CE=Ceará, TO=Tocantins, RN=Rio Grande do Norte, PB=Paraíba, PE=Pernambuco, AL=Alagoas, BA=Bahia, RJ=Rio de Janeiro, SP=São Paulo. Underlined states represent those from which sequences in this study were generated (upper inset). Publicly available sequences were also collated from non-underlined states. **b.** Confirmed and notified ZIKV cases in NE Brazil. Upper panel shows the temporal distribution of RT-qPCR+ cases detected during ZiBRA fieldwork. Only samples with known collection dates are included (n=138 out of 181 confirmed cases). Lower panel shows notified ZIKV cases in NE Brazil between 01 Jan 2015 and 19 Nov 2016 (n=122,779). The dashed line represents the average climatic vector suitability score for NE Brazil (**Methods**). The vertical arrow indicates date of ZIKV confirmation in NE Brazil/Americas<sup>1</sup>. **c.** Notified ZIKV cases in the Centre-West, Southeast, North, and South regions of Brazil (clockwise from top left). The dashed lines represent the average climatic vector suitability score for each region.

**Fig. 2. Zika virus genetic diversity and sequencing statistics.** **a.** The percentage of ZIKV genome sequenced plotted against RT-qPCR Ct-value, for each sample. Each circle represents a sequence recovered from an infected individual in Brazil and is coloured by sampling location. **b.** Illustration of sequencing coverage across the ZIKV genome for the ZiBRA sequences, including data generated by both mobile and static laboratories. **c.** Regression of sequence sampling dates against root-to-tip genetic distances in a maximum likelihood phylogeny of the Asian-ZIKV lineage. **Extended Data Fig. 2b** contains a comparable analysis that also includes P6-740 (the oldest Asian-ZIKV strain collected in 1966). **d.** Average pairwise genetic diversity of the PreAm-ZIKV strains (grey line) and of the Am-ZIKV lineage (black line), calculated using a sliding window of 300 nucleotides with a step size of 50 nucleotides.

**Fig. 3. Phylogeography of ZIKV in the Americas.** Maximum clade credibility phylogeny, estimated from complete and partial Am-ZIKV genomes using a molecular clock phylogeographic approach (**Methods**). Terminal branches with yellow circles indicate sequences reported in this study. Terminal branches with no circles and reduced opacity are those reported in a companion paper<sup>20</sup>. Thin vertical grey boxes indicate statistical uncertainty of estimated dates of nodes A, B and C (**Extended Data Table 3c**). Branch colours indicate the most probable ancestral lineage locations. Diamonds at internal nodes are sized in proportion to clade posterior probabilities. For selected nodes, coloured numbers show the posterior probabilities of ancestral locations and numbers in grey are clade posterior probabilities. Asterisks indicate the three available genomes from microcephaly cases. A black arrow indicates the oldest Brazilian ZIKV sequence. The grey arrow and dotted line denotes when ZIKV was first confirmed in the Americas<sup>1</sup>. Nodes A and B are equivalent to the nodes named identically in<sup>4</sup>. Text labels along the bottom of the figure denote clades of sequences from regions outside of NE Brazil. RJ1 to RJ4 are clades from Rio de Janeiro state, TO from Tocantins, and SP1 from São Paulo state. Clades from outside Brazil are denoted CB1 and CB2 (Caribbean), SA1 and SA2



483 (South America excluding Brazil), and CA1 (Central America). Thin grey horizontal  
484 lines along the bottom of the figure denote sequences from Brazil.

485  
486 **Fig. 4. Establishment of Am-ZIKV in the Americas.** The earliest inferred dates of  
487 lineage export to non-Brazilian regions, represented by box-and-whisker plots. Each  
488 plot corresponds to the earliest movement between a pair of locations with well-  
489 supported virus lineage migration. The first exports to South America outside Brazil  
490 (SA1 in **Fig. 3**), to Central America (CA1) and to the Caribbean (CB1) are shown in  
491 panels **a-c**, respectively. Box and whisker plots were generated in ggplot2, with boxes  
492 representing the median and interquartile ranges of the estimated date of earliest  
493 movement. In each of **a-c**, dashed lines show the estimated climatic vector suitability  
494 score for each recipient region, averaged across the countries for which sequence data  
495 is available (see **Methods**). In each of **a-c**, the bar plots show available notified ZIKV  
496 case data (plots adapted from PAHO) for the countries with the earliest confirmed  
497 cases (Colombia<sup>61</sup> in panel **a**, Mexico<sup>62</sup> in **b**, and Puerto Rico<sup>63</sup> in **c**). Coloured arrows  
498 indicate the earliest confirmation of ZIKV autochthonous cases in each non-Brazilian  
499 region. The vertical dashed line represents the date of ZIKV confirmation in the  
500 Americas.

501

Figure 1

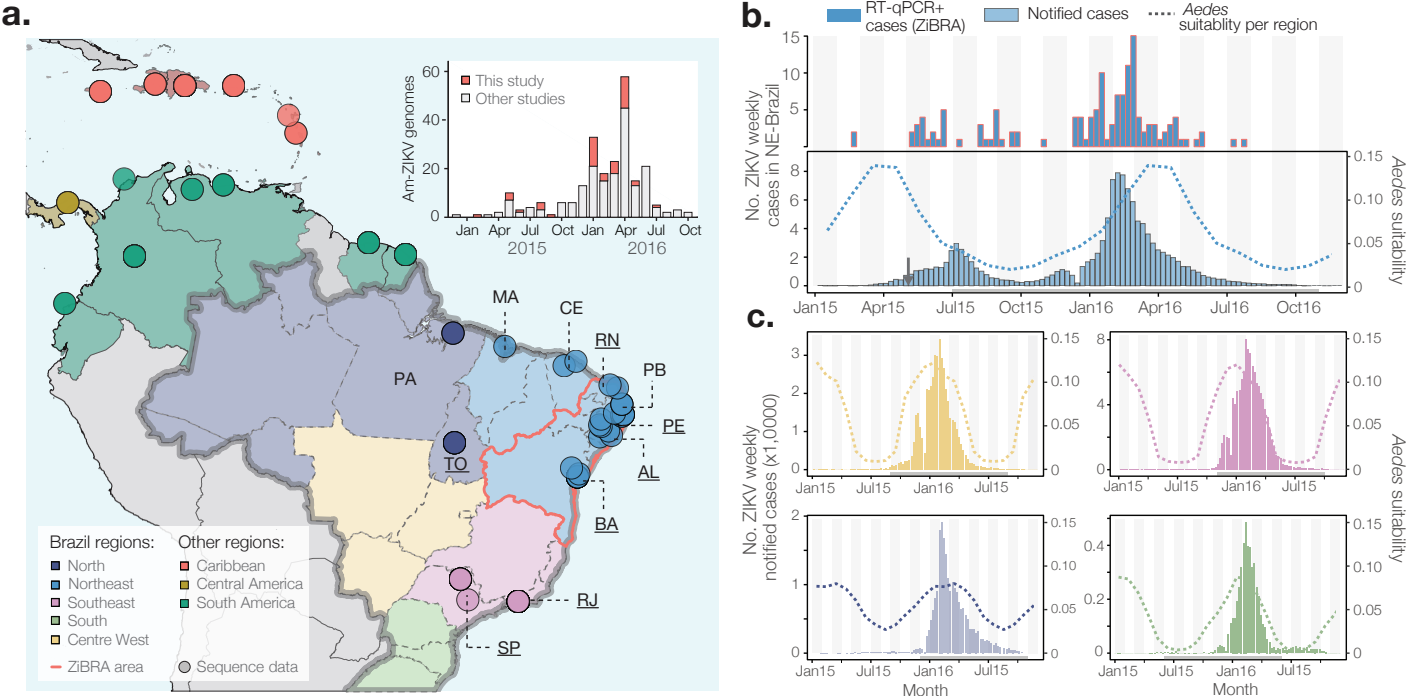


Figure 2

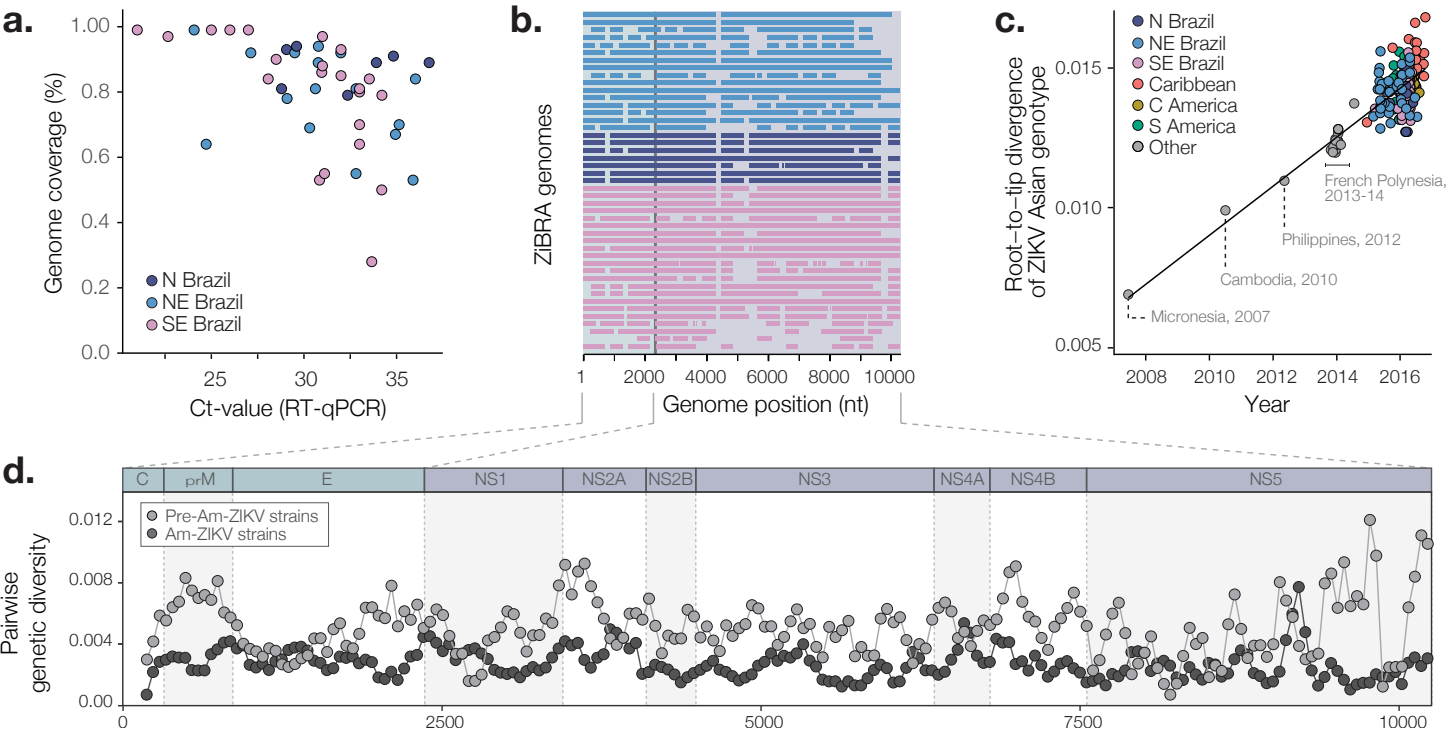


Figure 3

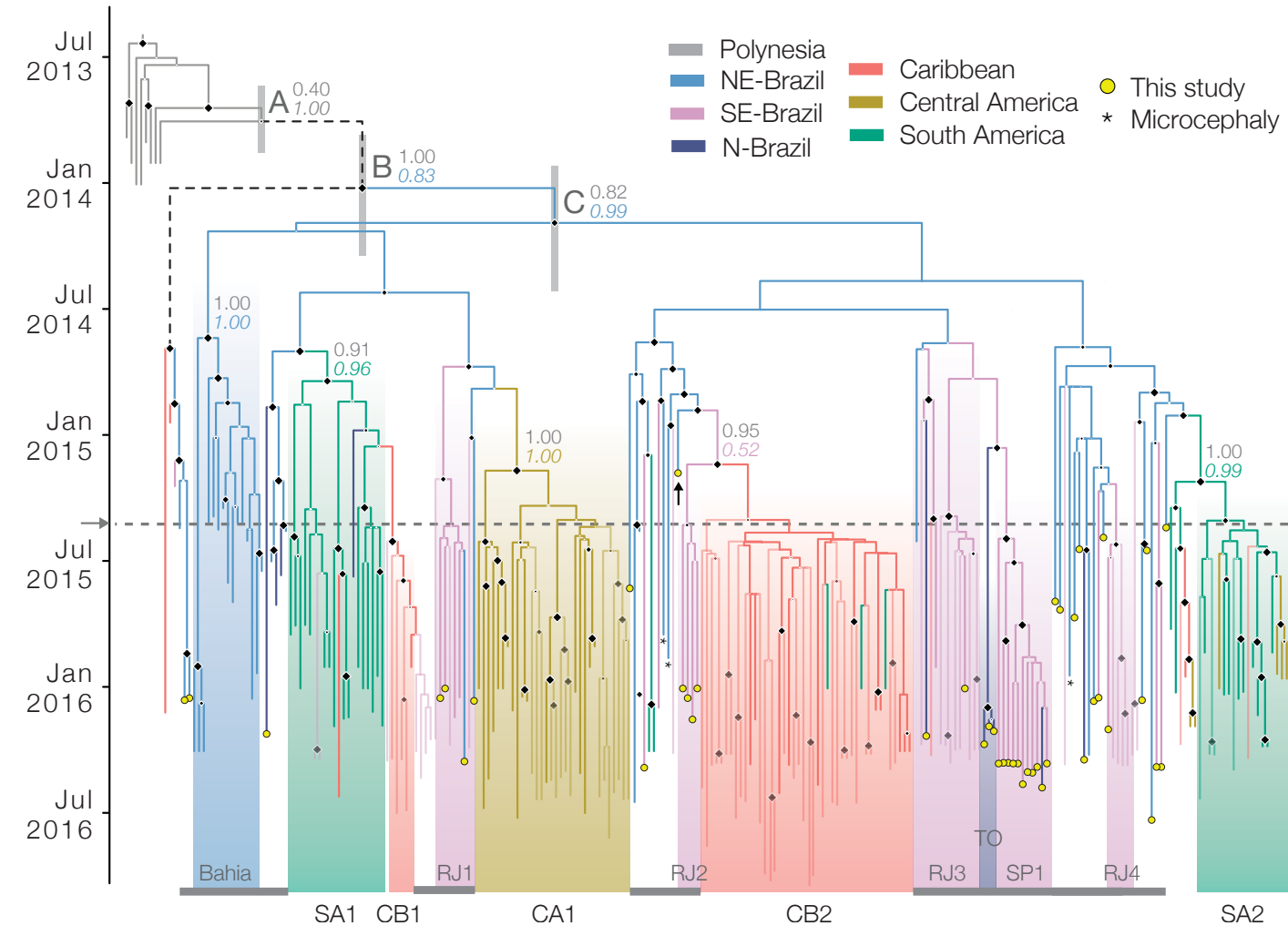
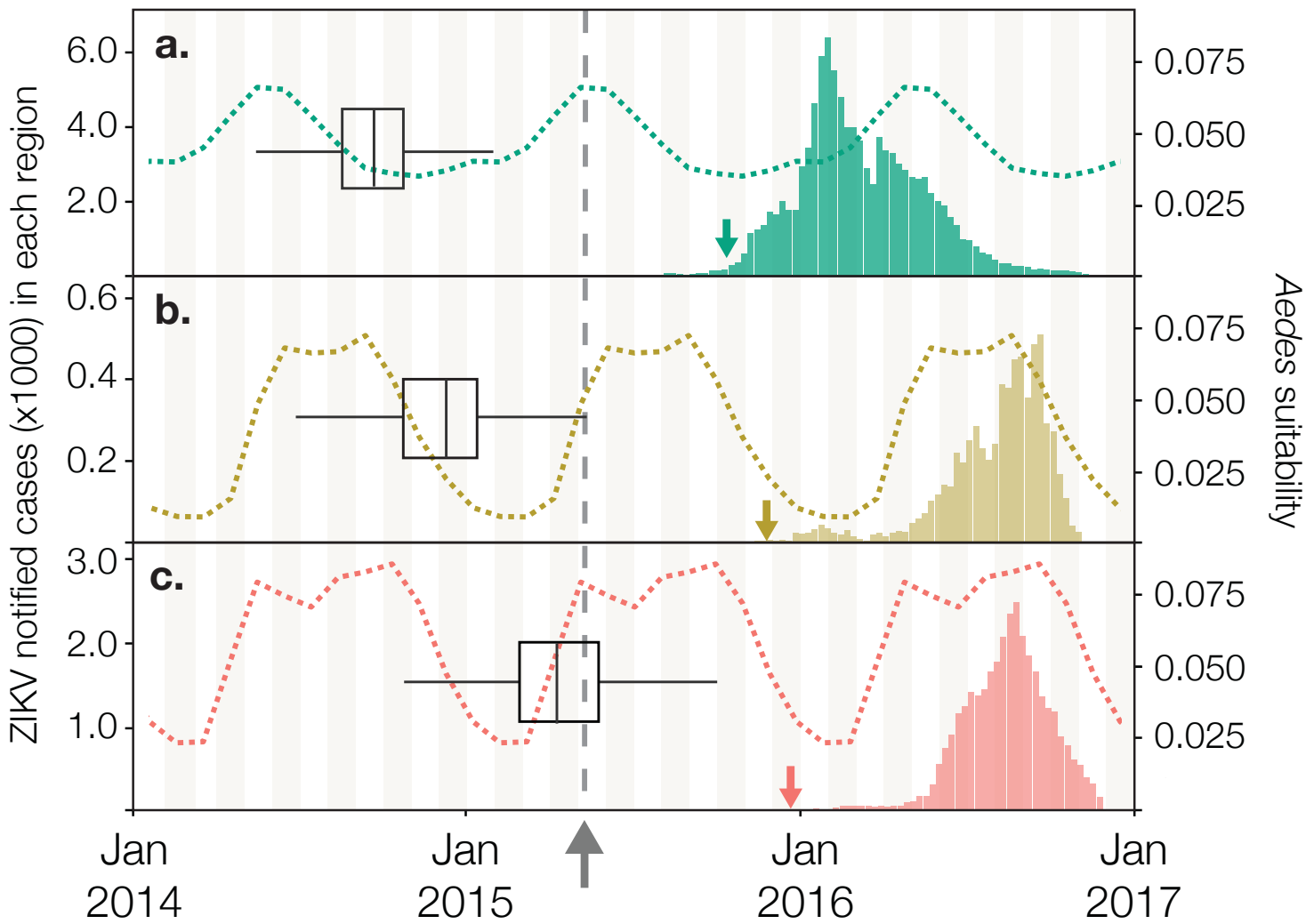


Figure 4



## 502 **Methods**

### 503 **Sample collection**

504 Between the 1<sup>st</sup> and 18<sup>th</sup> June 2016, 1330 samples from cases notified as ZIKV  
505 infected were tested for ZIKV infection in the Northeast region of Brazil (NE Brazil).  
506 During this period, 4 of the 5 laboratories in the region visited by the ZiBRA project  
507 were in the process of implementing molecular diagnostics for ZIKV. The ZiBRA  
508 team spent 2-3 days in each state central public health laboratory (LACEN). The  
509 samples analysed had been previously collected from patients who had attended a  
510 municipal or state public health facility, presenting maculopapular rash and at least  
511 two of the following symptoms: fever, conjunctivitis, polyarthralgia, or periarticular  
512 edema. The majority of samples were linked to a digital record that collated  
513 epidemiological and clinical data: date of sample collection, location of residence,  
514 demographic characteristics, and date of onset of clinical symptoms (when available).

515 The ZiBRA project was supported by the Brazilian Ministry of Health (MoH) as part  
516 of the emergency public health response to Zika. Samples had been previously  
517 obtained for routine diagnostic purposes from persons visiting local clinics by the  
518 Brazilian National Health Surveillance network as part of Zika virus surveillance  
519 activities. In these cases, we used samples without informed consent with the approval  
520 of the Brazilian Ministry of Health. Specifically, residual anonymized clinical  
521 diagnostic samples, with no or minimal risk to patients, were provided for research  
522 and surveillance purposes within the terms of Resolution 510/2016 of CONEP  
523 (Comissão Nacional de Ética em Pesquisa, Ministério da Saúde; National Ethical  
524 Committee for Research, Ministry of Health). For samples obtained from patients  
525 engaged in longitudinal studies of Zika virus in São Paulo and Tocantins states,  
526 informed consent was obtained (IRB CAAE 53153916.7.0000.0065). Samples from  
527 patients followed in Salvador and Feira de Santana were analysed under institutional  
528 approval from CPqGM/FioCruz/BA (1.184.454). Urine and plasma samples from Rio  
529 de Janeiro were obtained from patients at the Fiocruz Viral Hepatitis Ambulatory  
530 (Oswaldo Cruz Institute, Rio de Janeiro, Brazil) with Institutional Review Board  
531 approval (IRB142/01) from the Oswaldo Cruz Institute. RNA was extracted at the  
532 Paul-Ehrlich-Institut and sequenced at the University of Birmingham, UK.

### 534 **Nucleic acid isolation and RT-qPCR**

535 Serum, blood and urine samples were obtained from patients 0 to 228 days after first  
536 symptoms (**Extended Data Table 1a**). Viral RNA was isolated from 200 µl Zika-  
537 suspected samples using either the NucliSENS easyMag system (BioMerieux,  
538 Basingstoke, UK) (Ribeirão Preto samples), the ExiPrep Dx Viral RNA Kit  
539 (BIONEER, Republic of Korea) (Rio de Janeiro samples) or the QIAamp Viral RNA  
540 Mini kit (QIAGEN, Hilden, Germany) (all other samples) according to the  
541 manufacturer's instructions. Ct values were determined for all samples by probe-  
542 based RT-qPCR against the *prM* target (using 5'FAM as the probe reporter dye) as  
543 previously described<sup>34</sup>. RT-qPCR assays were performed using the QuantiNova Probe  
544 RT-qPCR Kit (20 µl reaction volume; QIAGEN) with amplification in the Rotor-  
545 Gene Q (QIAGEN) following the manufacturer's protocol. Primers/probe were  
546 synthesised by Integrated DNA Technologies (Leuven, Belgium). The following  
547 reaction conditions were used: reverse transcription (50°C, 10 min), reverse  
548 transcriptase inactivation and DNA polymerase activation (95°C, 20 sec), followed by  
549 40 cycles of DNA denaturation (95°C, 10 secs) and annealing-extension (60°C, 40

550 sec). Positive and negative controls were included in each batch; however, due to the  
551 large number of samples tested in a short time it was possible only to run each sample  
552 without replication.

553

#### 554 **Whole genome sequencing**

555 Sequencing was attempted on all positive samples obtained from NE Brazil regardless  
556 of Ct value. All samples collected in Brazil that are reported in this study were  
557 sequenced with the Oxford Nanopore MinION. Sequencing statistics can be found in  
558 **Extended Data Table 2**. The protocol employed cDNA synthesis with random  
559 primers followed by gene specific multiplex PCR and is presented in detail in Quick  
560 et al.<sup>18</sup>. In brief, extracted RNA was converted to cDNA using the Protoscript II First  
561 Strand cDNA synthesis Kit (New England Biolabs, Hitchin, UK) and random  
562 hexamer priming. ZIKV genome amplification by multiplex PCR was attempted  
563 using the ZikaAsianV1 primer scheme and 40 cycles of PCR using Q5 High-Fidelity  
564 DNA polymerase (NEB) as described in Quick et al.<sup>18</sup>. PCR products were cleaned-up  
565 using AmpureXP purification beads (Beckman Coulter, High Wycombe, UK) and  
566 quantified using fluorimetry with the Qubit dsDNA High Sensitivity assay on the  
567 Qubit 3.0 instrument (Life Technologies). PCR products for samples yielding  
568 sufficient material were barcoded and pooled in an equimolar fashion using the Native  
569 Barcoding Kit (Oxford Nanopore Technologies, Oxford, UK). Sequencing libraries  
570 were generated from the barcoded products using the Genomic DNA Sequencing Kit  
571 SQK-MAP007/SQK-LSK208 (Oxford Nanopore Technologies). Sequencing libraries  
572 were loaded onto a R9/R9.4 flowcell and data was collected for up to 48 hours but  
573 generally less. As described<sup>18</sup>, consensus genome sequences were produced by  
574 alignment of two-direction reads to a Zika virus reference genome (strain H/PF/2013,  
575 GenBank Accession number: KJ776791) followed by nanopore signal-level detection  
576 of single nucleotide variants. Only positions with  $\geq 20\times$  genome coverage were used to  
577 produce consensus alleles. Regions with lower coverage, and those in primer-binding  
578 regions were masked with N characters. Validation of our sequencing approach on the  
579 MinION platform was undertaken by using the MinION platform to sequence a WHO  
580 reference strain of Zika virus that was also sequenced using the Illumina Miseq  
581 platform<sup>19</sup>; identical consensus sequences were recovered regardless of the MinION  
582 chemistry version employed (R7.3, R9 and R9.4) (**Extended Data Fig. 1c**).

583

#### 584 **Collation of genome-wide data sets**

585 Our complete and partial genome sequences were appended to a global data set of all  
586 available published ZIKV genome sequences (up until January 2017) using an in-  
587 house script that retrieves updated GenBank sequences on a daily basis. In addition to  
588 the genomes generated from samples collected in NE Brazil during ZiBRA fieldwork,  
589 samples were sent directly to University of São Paulo and elsewhere for sequencing.  
590 Thirteen genomes from Ribeirão Preto, São Paulo state (SP; SE-Brazil region) and  
591 seven genomes from Tocantins (TO; N-Brazil region) were sequenced at University  
592 of São Paulo. Nine genomes from Rio de Janeiro (RJ; SE-Brazil region) were  
593 sequenced in Birmingham, UK, and added to our dataset. All these genomes were  
594 generated using the same primer scheme as the ZiBRA samples collected in NE  
595 Brazil<sup>18</sup>. In addition to these 45 sequences from Brazil, we further included in analysis  
596 9 genomes from ZIKV strains sampled outside of Brazil in order to contextualise the



genetic diversity of Brazilian ZIKV, giving rise to a final data set of 54 sequences. Specifically, we included 5 genomes from samples collected in Colombia and 4 new genomes from Mexico, which were generated using the protocols described in refs.<sup>35</sup> and<sup>22</sup>, respectively.

GenBank sequences belonging to the African genotype of ZIKV were identified using the Arboviral genotyping tool (<http://bioafrica2.mrc.ac.za/regagenotype/typingtool/aedesviruses>) and excluded from subsequent analyses, as our focus of study was the Asian genotype of ZIKV, and the Am-ZIKV lineage in particular. To assess the robustness of molecular clock dating estimates to the inclusion of older sequences, analyses were performed both with and without the P6-740 strain, the oldest known strain of the ZIKV-Asian genotype (sampled in 1966 in Malaysia). Our final alignment comprised the sequences reported in this study ( $n=54$ ) plus publicly available ZIKV-Asian genotype sequences, as of 1<sup>st</sup> March 2017 ( $n=115$ ). We also included in our analysis 85 additional genomes from a companion paper<sup>20</sup>. The dataset used for analysis therefore included sequences from 254 Zika virus isolates, 241 of which were from the Americas. Unpublished but publicly available genomes were included in our analysis only if we had written permission from those who generated the data (see **Acknowledgments**).

#### **Maximum likelihood analysis and recombination screening**

Preliminary maximum likelihood (ML) trees were estimated with ExaMLv3<sup>36</sup> using a per-site rate category model and a gamma distribution of among site rate variation. For the final analyses, ML trees were estimated using PhyML<sup>37</sup> under a GTR nucleotide substitution model<sup>38</sup>, with a gamma distribution of among site rate variation, as selected by jModeltest.v.2<sup>39</sup>. Branch support was inferred using 100 bootstrap replicates<sup>37</sup>. Final ML trees were estimated with NNI and SPR heuristic tree search algorithms; equilibrium nucleotide frequencies and substitution model parameters were estimated using ML<sup>37</sup> (see **Extended Data Fig. 3**).

Recombination may impact evolutionary estimates<sup>40</sup> and has been shown to be present in the ZIKV-African genotype<sup>41</sup>. In addition to restricting our analysis to the Asian genotype of ZIKV, we employed the 12 recombination detection methods available in RDPv4<sup>42</sup> and the Phi-test approach<sup>43</sup> available in SplitsTree<sup>44</sup> to further search for evidence of recombination in the ZIKV-Asian lineage. No evidence of recombination was found.

Analysis of the temporal molecular evolutionary signal in our ZIKV alignments was conducted using TempEst<sup>45</sup>. In brief, collection dates in the format yyyy-mm-dd (ISO 8601 standard) were regressed against root-to-tip genetic distances obtained from the ML phylogeny. When precise sampling dates were not available, a precision of 1 month or 1 year in the collection dates was taken into account.

To compare the pairwise genetic diversity of PreAm-ZIKV strains from Asia and the Pacific with Am-ZIKV viruses from the Americas, we used a sliding window approach with 300 nt wide windows and a step size of 50 nt. Sequence gaps were ignored; hence the average pairwise difference per window was obtained by dividing the total pairwise nucleotide differences by the total number of pairwise comparisons.

## 643 **Molecular clock phylogenetics and gene-specific $d_N/d_S$ estimation**

644 To estimate Bayesian molecular clock phylogenies, analyses were run in duplicate  
645 using BEASTv.1.8.4<sup>46</sup> for 30 million MCMC steps, sampling parameters and trees  
646 every 3000 steps. We employed a model selection procedure using both path-  
647 sampling and stepping stone models<sup>47</sup> to estimate the most appropriate combination of  
648 molecular clock and coalescent models for Bayesian phylogenetic analysis. The best  
649 fitting combination was a Bayesian skyline tree prior and a relaxed molecular clock  
650 model, with log-normally distributed variation in rates among branches (**Extended**  
651 **Data Table 3b**). A non-informative continuous time Markov chain reference prior<sup>49</sup>  
652 on the molecular clock rate was used. Convergence of MCMC chains was checked  
653 with Tracer v.1.6. After removal of burn-in, posterior tree distributions were  
654 combined and subsampled to generate an empirical distribution of 1,500 molecular  
655 clock trees.

656 To estimate rates of evolution per gene we partitioned the alignment into 10 genes (3  
657 structural genes *C*, *prM*, *E*, and 7 non-structural genes *NS1*, *NS2A*, *NS2B*, *NS3*, *NS4A*,  
658 *NS4B* and *NS5*) and employed a SDR06 substitution model<sup>48</sup> and a strict molecular  
659 clock model, using an empirical distribution of molecular clock phylogenies. To  
660 estimate the ratio of nonsynonymous to synonymous substitutions per site ( $d_N/d_S$ ) for  
661 the PreAm-ZIKV and the Am-ZIKV lineages, we used the single likelihood ancestor  
662 counting (SLAC) method<sup>50</sup> implemented in HyPhy<sup>51</sup>. This method was applied to two  
663 distinct codon-based alignments and their corresponding ML trees which comprised  
664 the PreAm-ZIKV and Am-ZIKV sequences, respectively.

665

## 666 **Phylogeographic analysis**

667 We investigated virus lineage movements using our empirical distribution of  
668 phylogenetic trees and the sampling location of each ZIKV sequence. The sampling  
669 location of sequences collected from returning travellers was set to the travel  
670 destination in the Americas where infection likely occurred. We discretised sequence  
671 sampling locations in Brazil into the geographic regions defined in the main text. The  
672 number of sequences per region available for analysis was 10 for N Brazil, 41 for NE  
673 Brazil and 54 for SE Brazil. No viral genetic data was available for the Centre-West  
674 (CW) and the South (S) Brazilian regions. We similarly discretised the locations of  
675 ZIKV sequences sampled outside of Brazil. These were grouped according to the  
676 United Nations M49 coding classification of macro-geographical regions. Our  
677 analysis included 53 sequences from the Caribbean, 38 from Central America, 17  
678 from Polynesia, 37 from South America (excluding Brazil), 3 from Southeast Asia  
679 and 1 from Micronesia. To account for the possibility of sampling bias arising from a  
680 larger number of sequences from particular locations, we repeated all  
681 phylogeographic analyses using (i) the full dataset ( $n=254$ ) and (ii) ten jackknife  
682 resampled datasets ( $n=74$ ) in which taxa from each location (except for Southeast  
683 Asia and Micronesia) were randomly sub-sampled to 10 sequences (the number of  
684 sequences available for N-Brazil).

685 Phylogeographic reconstructions were conducted using two approaches; (i) using the  
686 asymmetric<sup>52</sup> discrete trait evolution models implemented in BEASTv1.8.4<sup>46</sup> and (ii)  
687 using the Bayesian structured coalescent approximation (BASTA)<sup>29</sup> implemented in  
688 BEAST2v.2. The latter has been suggested to be less sensitive to sampling biases<sup>53</sup>.  
689 For both approaches, maximum clade credibility trees were summarized from the

MCMC samples using TreeAnnotator after discarding 10% as burn-in. The posterior estimates of the location of nodes A, B and C (depicted in **Fig. 3**) from these two analytical approaches (applied to both the complete and jackknifed data sets) can be found in **Extended Data Fig. 4**.

For the discrete trait evolution approach, we counted the expected number of transitions among each pair of locations (net migration) using the robust counting approach<sup>54,55</sup> available in BEASTv1.8.4<sup>46</sup>. We then used those inferred transitions to identify the earliest estimated ZIKV introductions into new regions. These viral lineage movement events were statistically supported (with Bayes factors > 3) using the BSSVS (Bayesian stochastic search variable selection) approach implemented in BEASTv.1.8.4<sup>30</sup>. Box plots for node ages were generated using the ggplot2<sup>56</sup> package in R software<sup>57</sup>.

### Epidemiological analysis

Weekly suspected ZIKV data per Brazilian region were obtained from the Brazilian Ministry of Health (MoH). Cases were defined as suspected ZIKV infection when patients presented maculopapular rash and at least two of the following symptoms: fever, conjunctivitis, polyarthralgia or periarticular edema. Because notified suspected ZIKV cases are based on symptoms and not molecular diagnosis, it is possible that some notified cases represent other co-circulating viruses with related symptoms, such as dengue and Chikungunya viruses. Further, case reporting may have varied among regions and through time. Data from 2015 came from the pre-existing MoH sentinel surveillance system that comprised 150 reporting units throughout Brazil, which was eventually standardised in Feb 2016 in response to the ZIKV epidemic. We suggest that these limitations should be borne in mind when interpreting the ZIKV notified case data and we consider the  $R_0$  values estimated here to be approximate. That said, our time series of RT-qPCR+ ZIKV diagnoses from NE Brazil qualitatively match the time series of notified ZIKV cases from the same region (**Fig. 1b**). To estimate the exponential growth rate of the ZIKV outbreak in Brazil, we fit a simple exponential growth rate model to each stage of the weekly number of suspected ZIKV cases from each region separately:

$$I_w = I_0 \exp(r_w \cdot w) \quad (1)$$

where  $I_w$  is the number of cases in week  $w$ . As described in main text, the Brazilian regions considered here were NE Brazil, N-Brazil, S-Brazil, SE-Brazil, and CW-Brazil. The time period over which exponential growth occurs was determined by plotting the log of  $I_w$  and selecting the period of linearity (**Extended Data Fig. 5**). A linear model was then fitted to this period to estimate the weekly exponential growth rate  $r_w$ :

$$\ln(I_w) = \ln(I_0) + r_w \cdot w \quad (2)$$

Let  $g(\cdot)$  be the probability density distribution of the epidemic generation time (i.e. the duration between the time of infection of a case and the mean time of infection of

its secondary infections). The following formula can be used to derive the reproduction number  $R$  from the exponential growth rate  $r$  and density  $g(\cdot)$ <sup>58</sup>.

737

$$R = \frac{1}{\int_0^{\infty} \exp(-r.t)g(t)dt} \quad (3)$$

In our baseline analysis, following Ferguson et al.<sup>59</sup> we assume that the ZIKV generation time is Gamma-distributed with a mean of 20.0 days and a standard deviation (SD) of 7.4 days. In a sensitivity analysis, we also explored scenarios with shorter mean generation times (10.0 and 15.0 days) but unchanged coefficient of variation  $SD/mean=7.4/20=0.37$  (**Extended Data Table 1c**).

744

#### 745 **Association between *Aedes aegypti* climatic suitability and ZIKV notified cases**

To account for seasonal variation in the geographical distribution of the ZIKV vector *Aedes aegypti* in Brazil we fitted high-resolution maps<sup>60</sup> to monthly covariate data. Covariate data included time-varying variables, such as temperature-persistence suitability, relative humidity, and precipitation, as well as static covariates such as urban versus rural land use. Maps were produced at a 5km x 5km resolution for each calendar month and then aggregated to the level of the five Brazilian regions used in this study (**Extended Data Fig. 6**). For consistency, we rescaled monthly suitability values so that the sum of all monthly maps equalled the annual mean map<sup>9</sup>.

We then assessed the correlation between monthly *Aedes aegypti* climatic suitability and the number of weekly ZIKV notified cases in each Brazilian region, to test how well vector suitability explains the variation in the number of ZIKV notified cases. To account for the correlation in each Brazilian region we fit a linear regression model with a lag and two breakpoints. As there may be a lag between trends in suitability and trends in notified cases, we include a temporal term in the model to allow for a shift in the respective curves. Thus for each region, different sets of the constant and linear terms are fitted to different time periods. More formally,

762

$$\log(y_i + 1) = \alpha + \mathbb{I}(i \notin T)\alpha' + [b + \mathbb{I}(i \notin T)b']x_{i-l} \quad (4)$$

764

where  $y_i$  represents notified cases in a particular region in month  $i$ ,  $x_i$  is the climatic suitability in that region in month  $i$ ,  $l$  is the time lag that yields the highest correlation between  $y_i$  and  $x_i$  and  $T$  is the set of time indexes in the correlated region.

We then find the values of  $T$  and  $l$  that provide the highest adjusted- $R^2$  by stepwise iterative optimisation. For each value of  $T$  evaluated, the optimal value of  $l$  (i.e. that which gives the highest adjusted- $R^2$  for the model above) is found by the optim function in  $R$ <sup>57</sup>. Climatic suitability values were only calculated for each month, so to calculate suitability values for any given point in time we interpolated between the monthly values using a linear function. We found no significant effect of residual autocorrelation in our data (**Extended Data Fig. 7**).

775

776

777

## 778 Data availability

779 Sequences of the primers and probes used here have been available at  
 780 <http://www.zibraproject.org> since the beginning of the project. XML files and datasets  
 781 analysed in this study are available from the same website. New Brazilian sequences  
 782 are available in GenBank under accession numbers KY558989 to KY559032 and  
 783 KY817930. New Colombian and Mexican sequences are available under accession  
 784 numbers KY317936-40 and KY606271-4, respectively. See **Extended Data Table 2**  
 785 for further details.

786

787

- 788 34 Lanciotti, R. S. *et al.* Genetic and serologic properties of Zika virus associated  
 789 with an epidemic, Yap State, Micronesia, 2007. *Emerging Infectious Diseases*  
 790 **14**, 1232-1239, doi:10.3201/eid1408.080287 (2008).
- 791 35 Grubaugh, N. D. *et al.* Multiple introductions of Zika virus into the United  
 792 States revealed through genomic epidemiology. *bioRxiv*  
 793 <https://doi.org/10.1101/104794> (2017).
- 794 36 Kozlov, A. M., Aberer, A. J., Stamatakis, A. ExaML version 3: a tool for  
 795 phylogenomic analyses on supercomputers. *Bioinformatics* **31**, 2577-2579  
 796 (2015).
- 797 37 Guindon, S. *et al.* New algorithms and methods to estimate maximum-  
 798 likelihood phylogenies: assessing the performance of PhyML 3.0. *Systematic*  
 799 *Biology* **59**, 307-321, doi:10.1093/sysbio/syq010 (2010).
- 800 38 Hasegawa, M., Kishino, H. & Yano, T. Dating of the human-ape splitting by a  
 801 molecular clock of mitochondrial DNA. *Journal of Molecular Evolution* **22**,  
 802 160-174 (1985).
- 803 39 Darriba, D., Taboada, G. L., Doallo, R. & Posada, D. jModelTest 2: more  
 804 models, new heuristics and parallel computing. *Nature Methods* **9**, 772,  
 805 doi:10.1038/nmeth.2109 (2012).
- 806 40 Schierup, M. H. & Hein, J. Consequences of recombination on traditional  
 807 phylogenetic analysis. *Genetics* **156**, 879-891 (2000).
- 808 41 Faye, O. *et al.* Molecular evolution of Zika virus during its emergence in the  
 809 20(th) century. *PLoS Negl Trop Dis* **8**, e2636,  
 810 doi:10.1371/journal.pntd.0002636 (2014).
- 811 42 Martin, D. P., Murrell, B., Golden, M., Khoosal, A. & Muhire, B. RDP4:  
 812 Detection and analysis of recombination patterns in virus genomes. *Virus Evol*  
 813 **1**, vev003, doi:10.1093/ve/vev003 (2015).
- 814 43 Bruen, T. C., Philippe, H. & Bryant, D. A simple and robust statistical test for  
 815 detecting the presence of recombination. *Genetics* **172**, 2665-2681,  
 816 doi:10.1534/genetics.105.048975 (2006).
- 817 44 Huson, D. H. & Bryant, D. Application of phylogenetic networks in  
 818 evolutionary studies. *Molecular Biology and Evolution* **23**, 254-267,  
 819 doi:10.1093/molbev/msj030 (2006).
- 820 45 Rambaut, A., Lam, T. T., Fagundes de Carvalho, L., Pybus, O. G. Exploring  
 821 the temporal structure of heterochronous sequences using TempEst (formerly  
 822 Path-O-Gen). *Virus Evolution* **2** (2016).
- 823 46 Drummond, A. J., Suchard, M. A., Xie, D. & Rambaut, A. Bayesian  
 824 phylogenetics with BEAUti and the BEAST 1.7. *Molecular Biology and*  
 825 *Evolution* **29**, 1969-1973, doi:10.1093/molbev/mss075 (2012).

826 47 Baele, G., Li, W. L., Drummond, A. J., Suchard, M. A. & Lemey, P. Accurate  
827 model selection of relaxed molecular clocks in bayesian phylogenetics.  
828 *Molecular Biology and Evolution* **30**, 239-243, doi:10.1093/molbev/mss243  
829 (2013).

830 48 Shapiro, B., Rambaut, A. & Drummond, A. J. Choosing appropriate  
831 substitution models for the phylogenetic analysis of protein-coding sequences.  
832 *Molecular Biology and Evolution* **23**, 7-9, doi:10.1093/molbev/msj021 (2006).

833 49 Ferreira, M. A. R. & Suchard, M. A. Bayesian analysis of elapsed times in  
834 continuous-time Markov chains. *Can J Stat* **36**, 355-368 (2008).

835 50 Kosakovsky Pond, S. L., Frost, S. D. Not so different after all: a comparison  
836 of methods for detecting amino acid sites under selection. *Molecular Biology  
837 and Evolution* **22**, 1208-1222 (2005).

838 51 Pond, S. L., Frost, S. D. & Muse, S. V. HyPhy: hypothesis testing using  
839 phylogenies. *Bioinformatics* **21**, 676-679, doi:10.1093/bioinformatics/bti079  
840 (2005).

841 52 Edwards, C. J. *et al.* Ancient hybridization and an Irish origin for the modern  
842 polar bear matriline. *Current Biology : CB* **21**, 1251-1258,  
843 doi:10.1016/j.cub.2011.05.058 (2011).

844 53 Bouckaert, R. *et al.* BEAST 2: a software platform for Bayesian evolutionary  
845 analysis. *PLoS Computational Biology* **10**, e1003537,  
846 doi:10.1371/journal.pcbi.1003537 (2014).

847 54 Minin, V. N. & Suchard, M. A. Fast, accurate and simulation-free stochastic  
848 mapping. *Philos Trans R Soc Lond B Biol Sci* **363**, 3985-3995,  
849 doi:10.1098/rstb.2008.0176 (2008).

850 55 O'Brien, J. D., Minin, V. N. & Suchard, M. A. Learning to count: robust  
851 estimates for labeled distances between molecular sequences. *Molecular  
852 Biology and Evolution* **26**, 801-814, doi:10.1093/molbev/msp003 (2009).

853 56 Wickham, H. *ggplot2: elegant graphics for data analysis*. (Springer New  
854 York, 2009).

855 57 R: A Language and Environment for Computing (R Foundation for Statistical  
856 Computing, Vienna, Austria, 2014).

857 58 Cori, A., Ferguson, N. M., Fraser, C. & Cauchemez, S. A new framework and  
858 software to estimate time-varying reproduction numbers during epidemics.  
859 *American Journal of Epidemiology* **178**, 1505-1512, doi:10.1093/aje/kwt133  
860 (2013).

861 59 Ferguson, N. M. *et al.* EPIDEMIOLOGY. Countering the Zika epidemic in  
862 Latin America. *Science* **353**, 353-354, doi:10.1126/science.aag0219 (2016).

863 60 Kraemer, M. U. *et al.* The global distribution of the arbovirus vectors *Aedes  
864 aegypti* and *Ae. albopictus*. *eLife* **4**, e08347, doi:10.7554/eLife.08347 (2015).

865 61 PAHO/WHO. Zika Epidemiological Update - Colombia (21 Dec 2016).  
866 (Washington, D. C., 2016).

867 62 PAHO/WHO. Zika Epidemiological Update - Mexico (20 Dec 2016).  
868 (Washington, D. C., 2016).

869 63 PAHO/WHO. Zika Epidemiological Update - Puerto Rico (20 Dec 2016).  
870 (Washington, D. C., 2016).

## 873 Extended Data Figure Legends

874 **Extended Data Fig. 1. a.** The distribution of CT-values for the RT-qPCR+ samples  
875 tested during the ZiBRA journey in Brazil ( $n=181$  samples; median CT = 35.96). **b.**  
876 shows the distribution of the temporal lag between the date of onset of clinical  
877 symptoms and the date of sample collection of RT-qPCR+ samples (median lag = 2  
878 days). Red dashed lines represent the median of the distributions. **(c)** Validation of  
879 sequencing approaches. A phylogeny of the ZIKV Asian genotype estimated using  
880 PhyML<sup>37</sup> is shown. The expanded clade highlighted in blue contains the WHO  
881 reference ZIKV sequence<sup>19</sup> (accession number KX369547), which was generated  
882 using Illumina MiSeq. Sequences generated using MinION chemistries R9.4 2D, R9.4  
883 1D, R9 1D, R9 2D and R7.3 2D contain no nucleotide differences and hence were  
884 also placed in this clade. Scale bars represent expected nucleotide substitutions per  
885 site (s/s). Am-ZIKV=American Zika virus lineage.

886  
887 **Extended Data Fig. 2.** Temporal signal of the ZIKV Asian genotype. The correlation  
888 between sampling dates and genetic distances from the tips to the root of a maximum  
889 likelihood (ML) tree, estimated using PhyML<sup>37</sup>, was explored using TempEst<sup>45</sup>. **a.**  
890 Estimates for the dataset used in the phylogenetic analysis presented in **Fig. 3c**, and **b.**  
891 estimates for the same dataset with the addition of the P6-740 strain sampled in 1966  
892 (accession number HQ234499).

893  
894 **Extended Data Fig. 3.** A non-clock maximum likelihood phylogeny of our ZIKV  
895 data set. Bootstrap branch support values are shown at each node. The phylogeny was  
896 estimated using PhyML<sup>37</sup>. Sequences generated in this study are highlighted in red.  
897 Scale bar represents expected nucleotide substitutions per site.

898  
899 **Extended Data Fig. 4.** Ancestral node location posterior probabilities (ANLPP), for  
900 nodes A, B and C, estimated using the complete dataset (top row) and ten replicate  
901 subsampled data sets (other rows). See **Methods** for details. ANLPPs were calculated  
902 using two approaches: DTA=discrete trait analysis method<sup>30</sup> (left side columns) and  
903 BASTA=Bayesian structured coalescent approximation method<sup>29</sup> (right side  
904 columns). For each method, we employed an asymmetric model of location exchange  
905 to estimate ancestral node locations and to infer patterns of virus spread among  
906 regions.

907  
908 **Extended Data Fig. 5.** Epidemic growth rates estimated from weekly ZIKV notified  
909 cases in Brazil. Time series show the number of ZIKV notified cases in each region of  
910 Brazil. Periods from which exponential growth were estimated are highlighted in  
911 grey.

912  
913 **Extended Data Fig. 6.** Seasonal suitability for ZIKV transmission in the Americas.  
914 These maps were estimated by collating data on *Aedes* mosquitoes, temperature,  
915 relative humidity and precipitation, and are the basis of the trends in suitability for  
916 different regions shown in main text **Figs. 1 and 4**. For method details, see <sup>9,60</sup>.

917  
918 **Extended Data Fig. 7.** Partial autocorrelation functions for the linear model  
919 associating climatic suitability and ZIKV notified cases in each geographic region in  
920 Brazil. The residuals for the North, Northeast, Centre-West and Southeast regions  
921 show no autocorrelation, while a small amount of autocorrelation cannot be excluded  
922 for the South region.



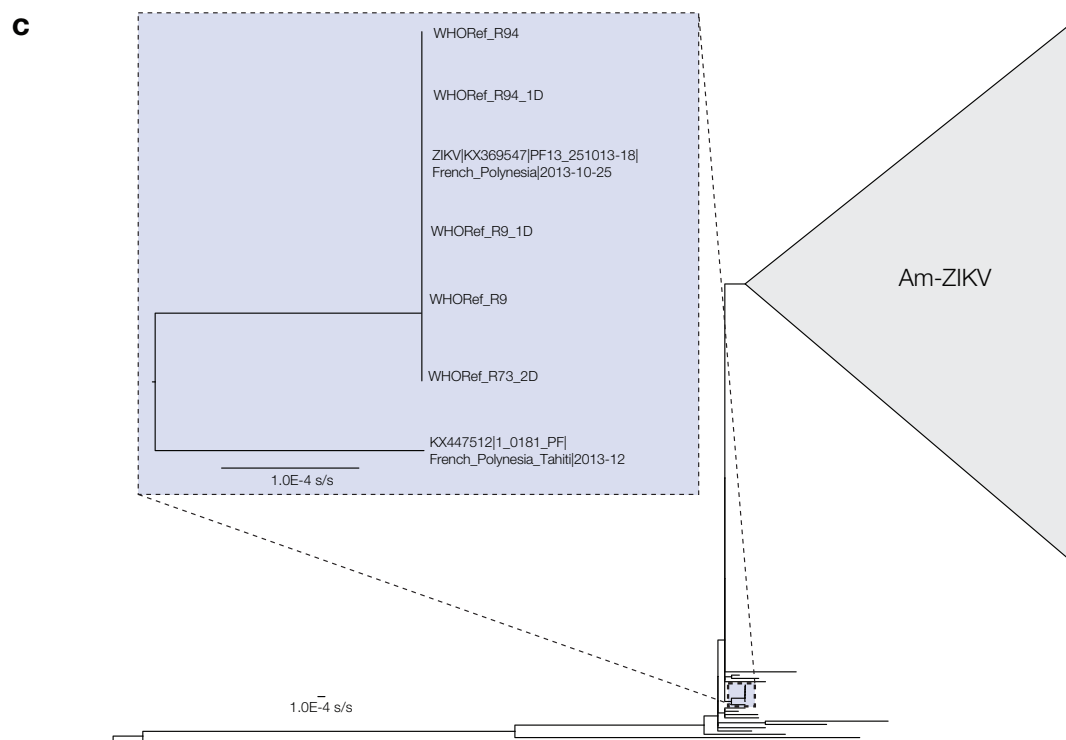
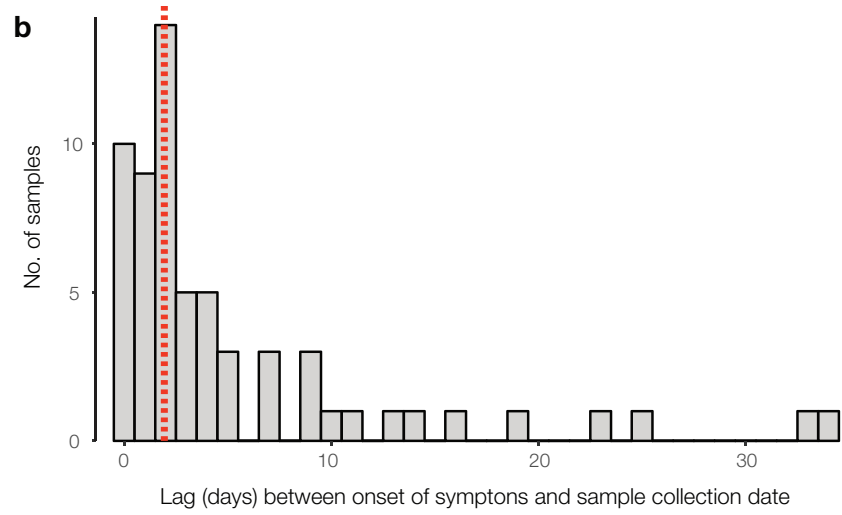
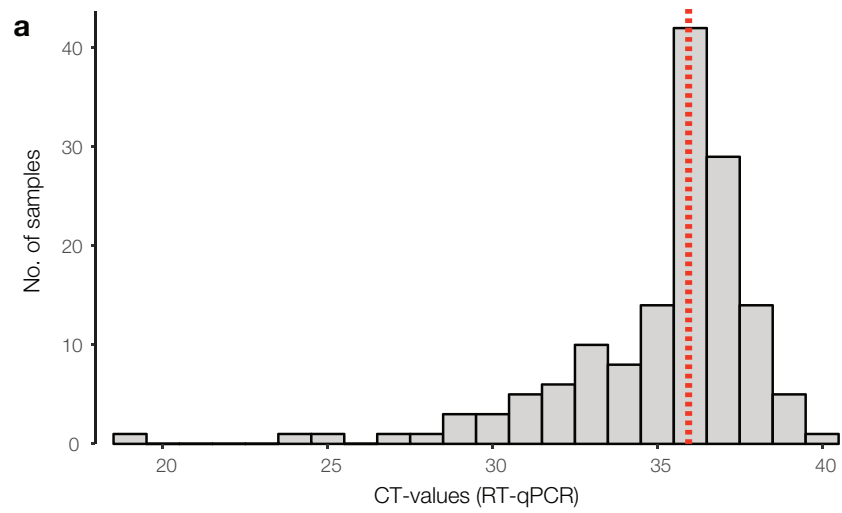
## 923 Extended Data Table Legends

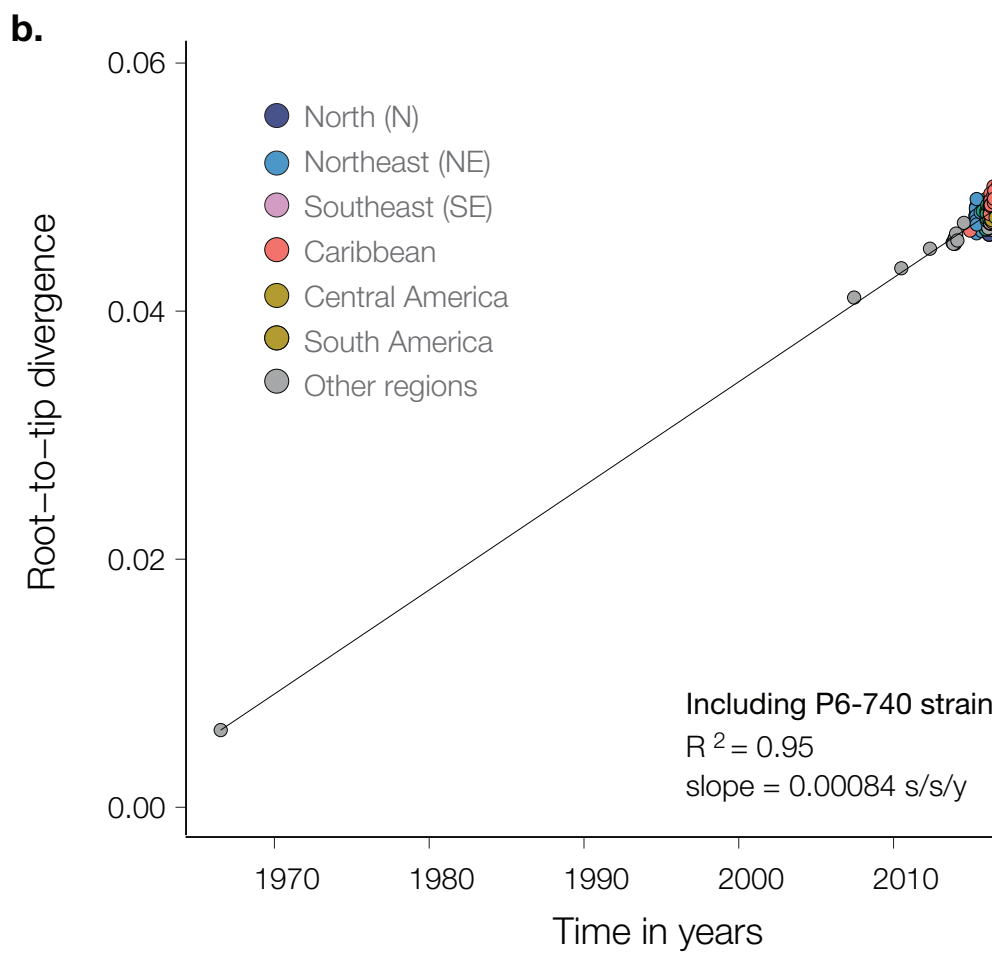
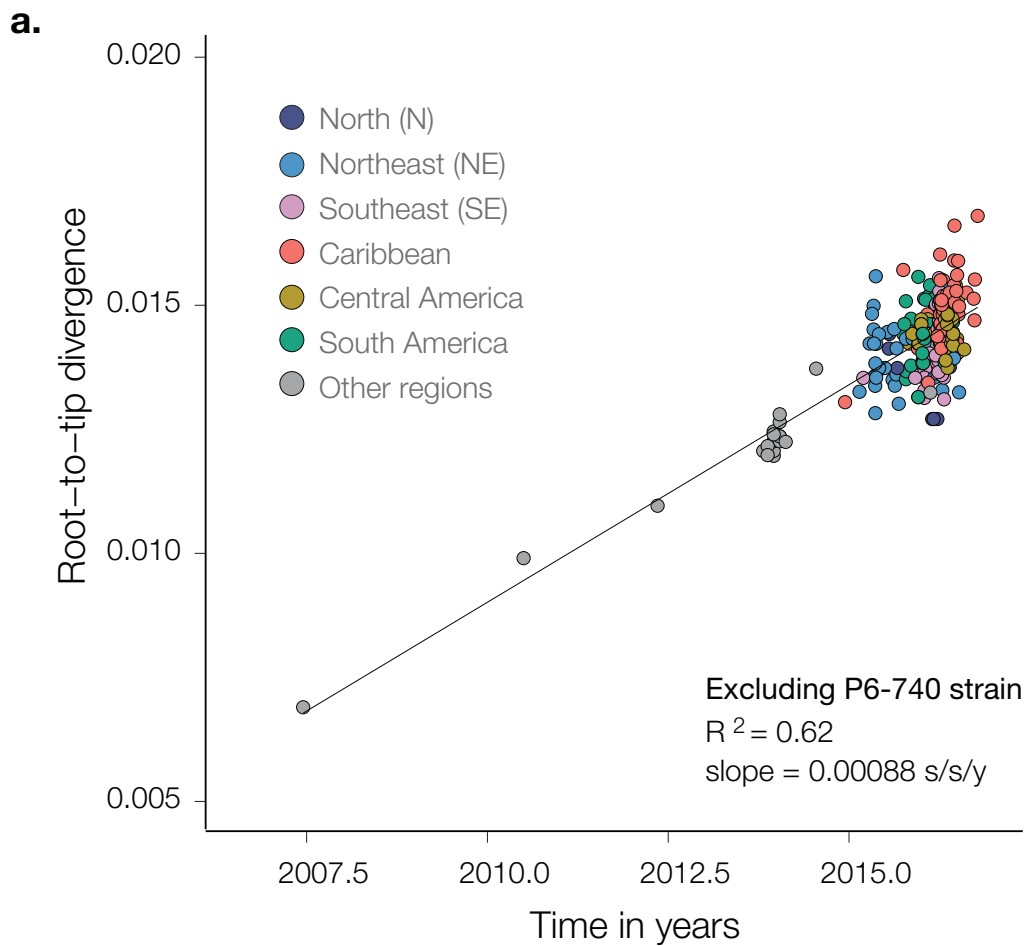
924 **Extended Data Table 1. a.** Summary of the clinical samples tested ( $n=1330$ , of  
 925 which 181 were RT-qPCR+) by the ZiBRA mobile lab in June 2016, NE Brazil. 84%  
 926 of samples with known collection dates ( $n=698$  of 826) were from 2016. ZIKV  
 927 notified cases were confirmed using RT-qPCR (see **Methods**). Collection lag  
 928 represents the median time interval (in days) between the date of onset of clinical  
 929 symptoms and date of sample collection (both dates available for  $n=219$ ) for all  
 930 samples (including those that subsequently tested RT-qPCR negative). Federal states  
 931 are RN: Rio Grande do Norte, PB: Paraíba, PE: Pernambuco, AL: Alagoas, BA:  
 932 Bahia. Sample numbers in the FioCruz, PE row include RT-PCR+ cases from  
 933 Pernambuco generated at Fiocruz Pernambuco. **b.** Parameters of the model  
 934 measuring the link between climatic vector suitability and notified ZIKV cases in  
 935 different Brazilian regions (CW: Centre-West, N: North, NE: Northeast, SE:  
 936 Southeast, S: South). For each region, the table provides the estimated correlated  
 937 time period ( $T$ ), P-value of the linear term of suitability in  $T$ , adjusted- $R^2$  of the  
 938 model, and time lag ( $l$ ). **c.** For each region, estimates of the basic reproductive  
 939 number ( $R$ ) of ZIKV are shown for several values of generation time ( $g$ ) parameter,  
 940 together with the corresponding estimates of exponential growth rate ( $r$ ) (per day)  
 941 obtained from notified ZIKV case counts (see Extended Data Fig. 7). 1<sup>st</sup>: epidemic  
 942 wave in 2015; 2<sup>nd</sup>: epidemic wave in 2016.

943  
 944 **Extended Data Table 2.** Sequencing statistics. Accession numbers, sample IDs,  
 945 sequencing coverage, RT-qPCR values and epidemiological information for the  
 946 samples from Brazil generated in this study. For the sequences from RJ state,  
 947 alignments were performed against version 2 (KJ776791.2) of the genome reference;  
 948 all other sequences used version 1 (KJ776791.1).

949  
 950 **Extended Data Table 3. a.** Estimated per-gene rates of evolution (mean and 95%  
 951 Bayesian credible intervals=BCIs) are shown in units of  $10^{-3}$  substitutions per site per  
 952 year. **b.** Log-marginal likelihood estimates using the path-sampling (PS) and  
 953 Stepping-Stone (SS) model selection approaches<sup>47</sup>. The overall ranking of the models  
 954 is shown in parentheses for each estimator and the best-fitting combination is  
 955 underscored. Two molecular clock models were tested here. SC: Strict clock model,  
 956 UCLN: uncorrelated relaxed clock with lognormal distribution<sup>46</sup>. **c.** Estimated dates  
 957 of nodes A, B and C (**Fig. 3**) under various different molecular clock and coalescent  
 958 model combinations. TMRCA: time of the most recent common ancestor, BCI:  
 959 Bayesian credible interval, SC: strict molecular clock model, UCLN: uncorrelated  
 960 clock with lognormal distribution.

961

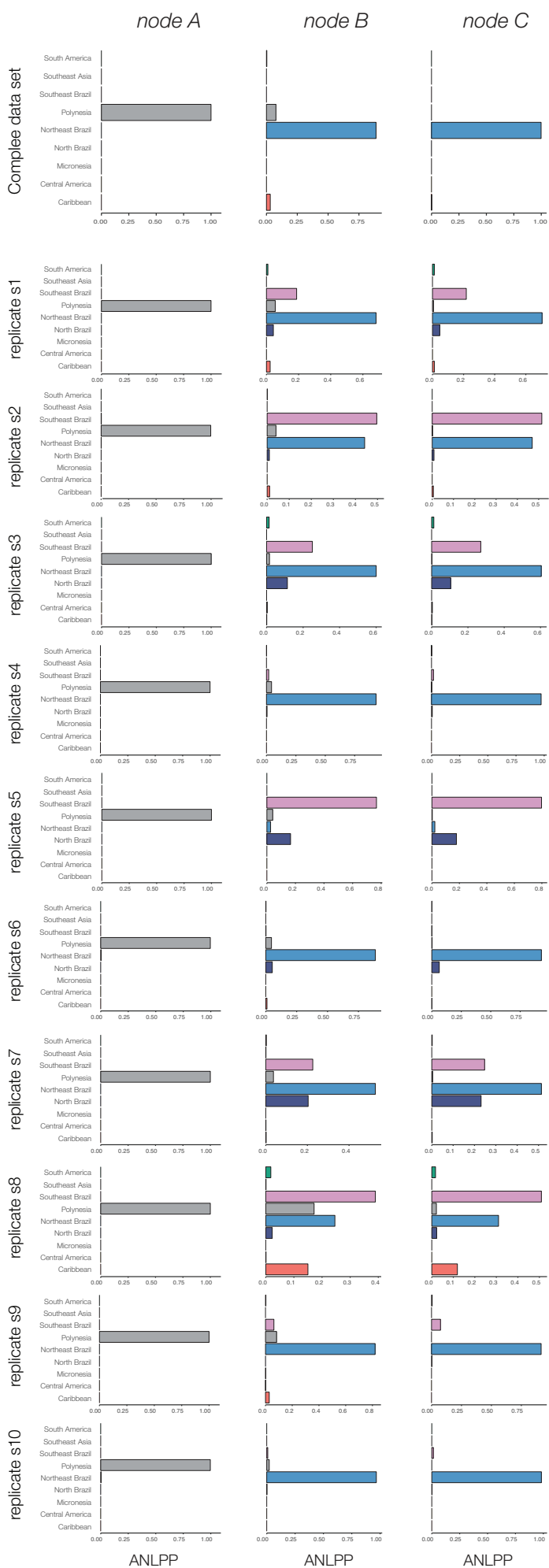




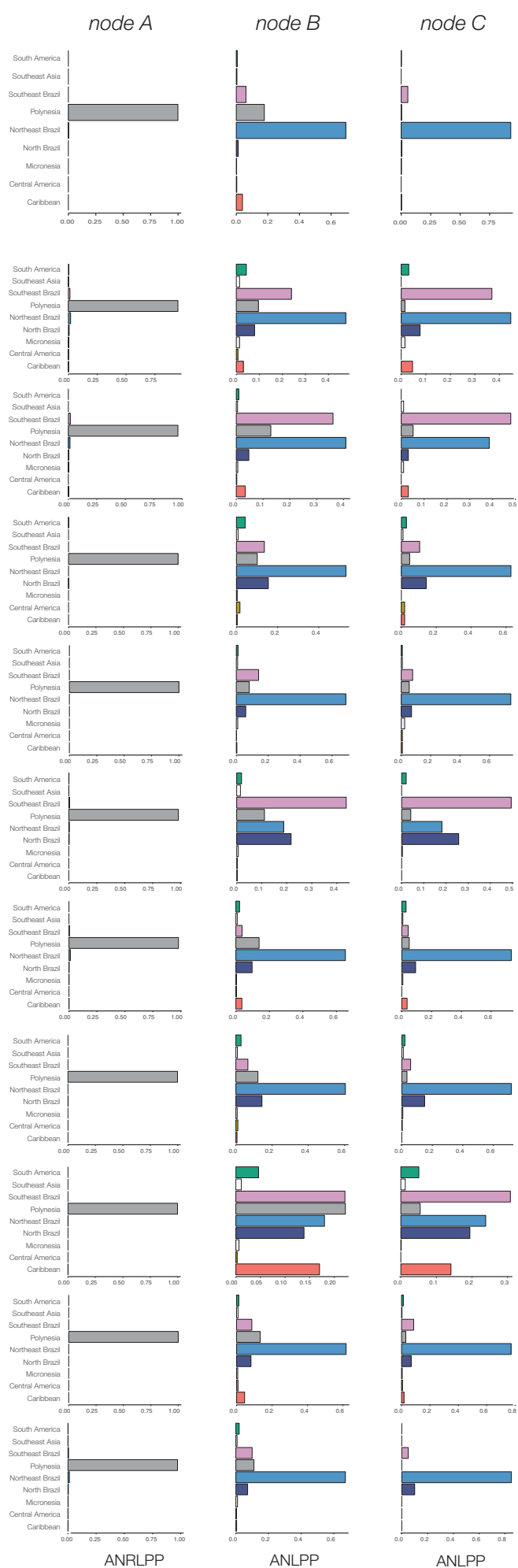


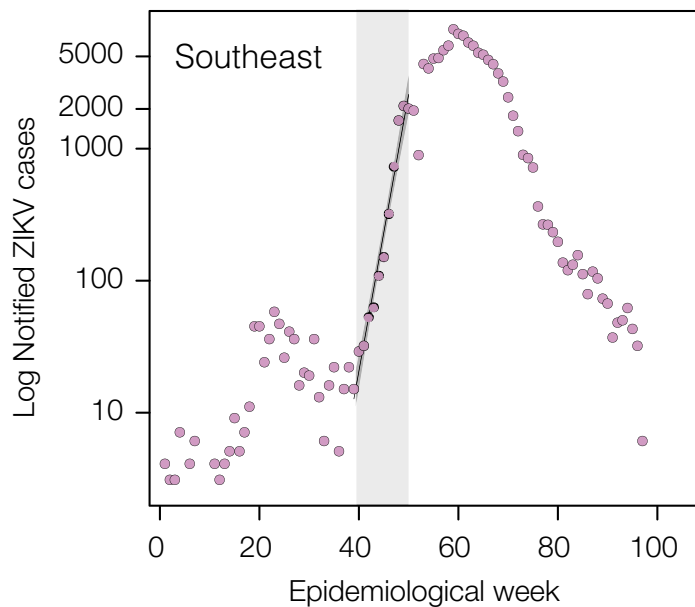
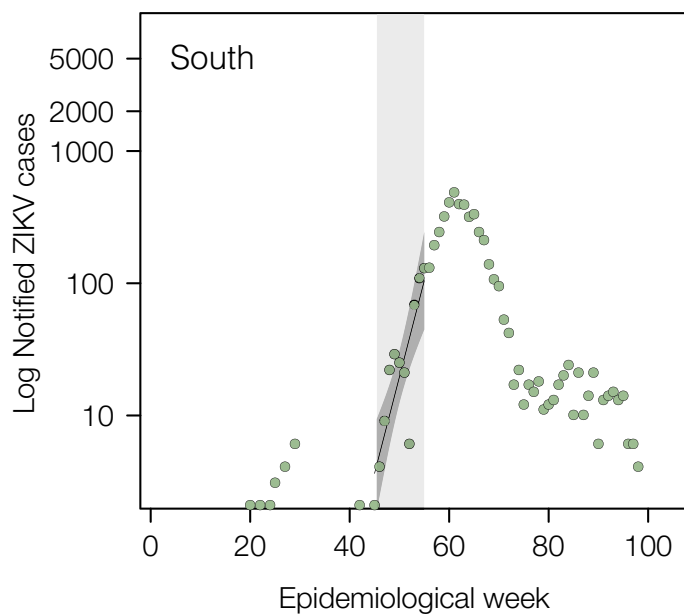
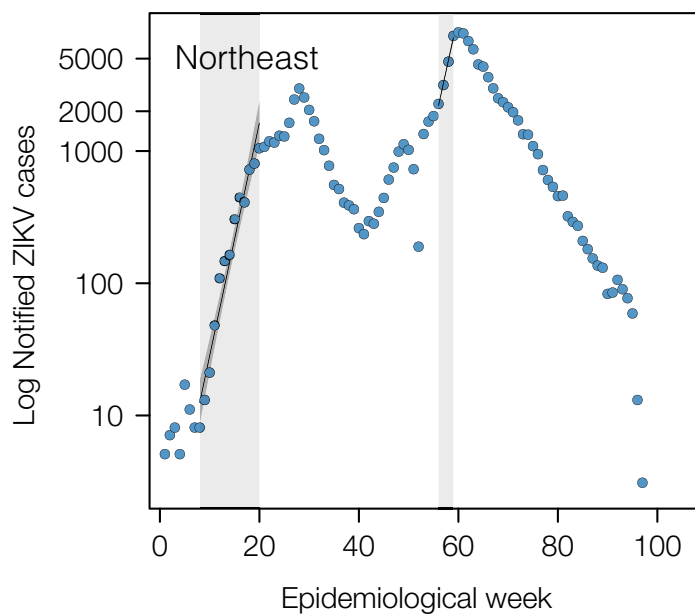
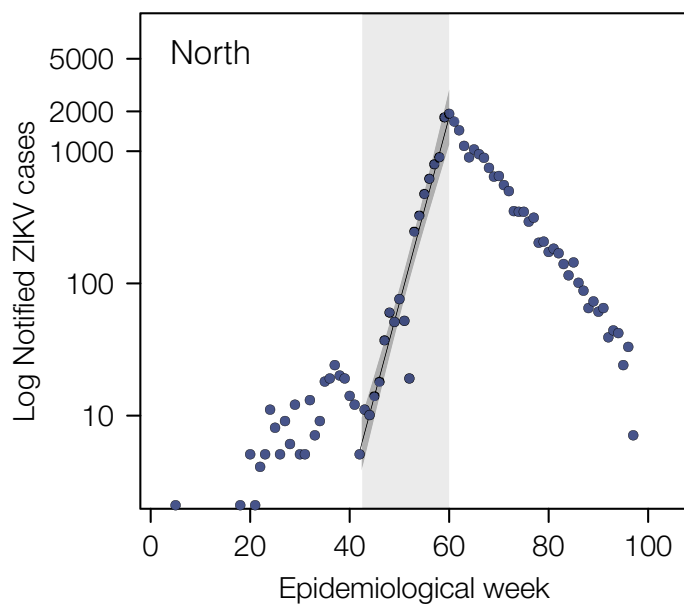
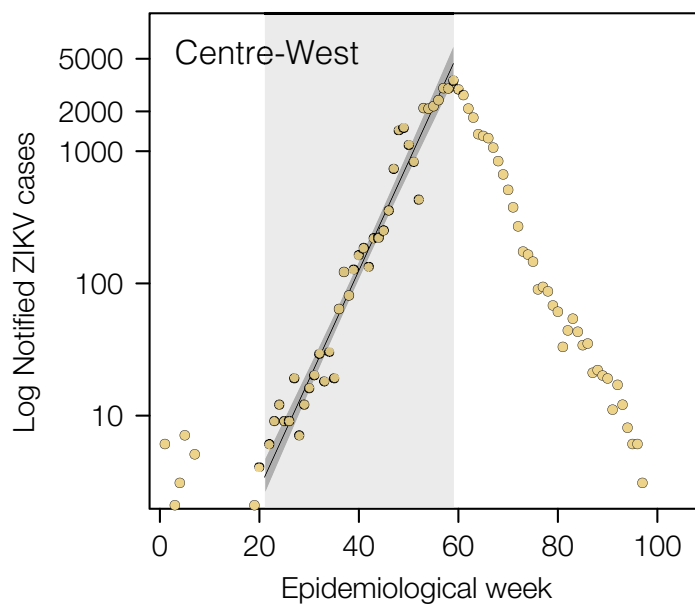
0.002

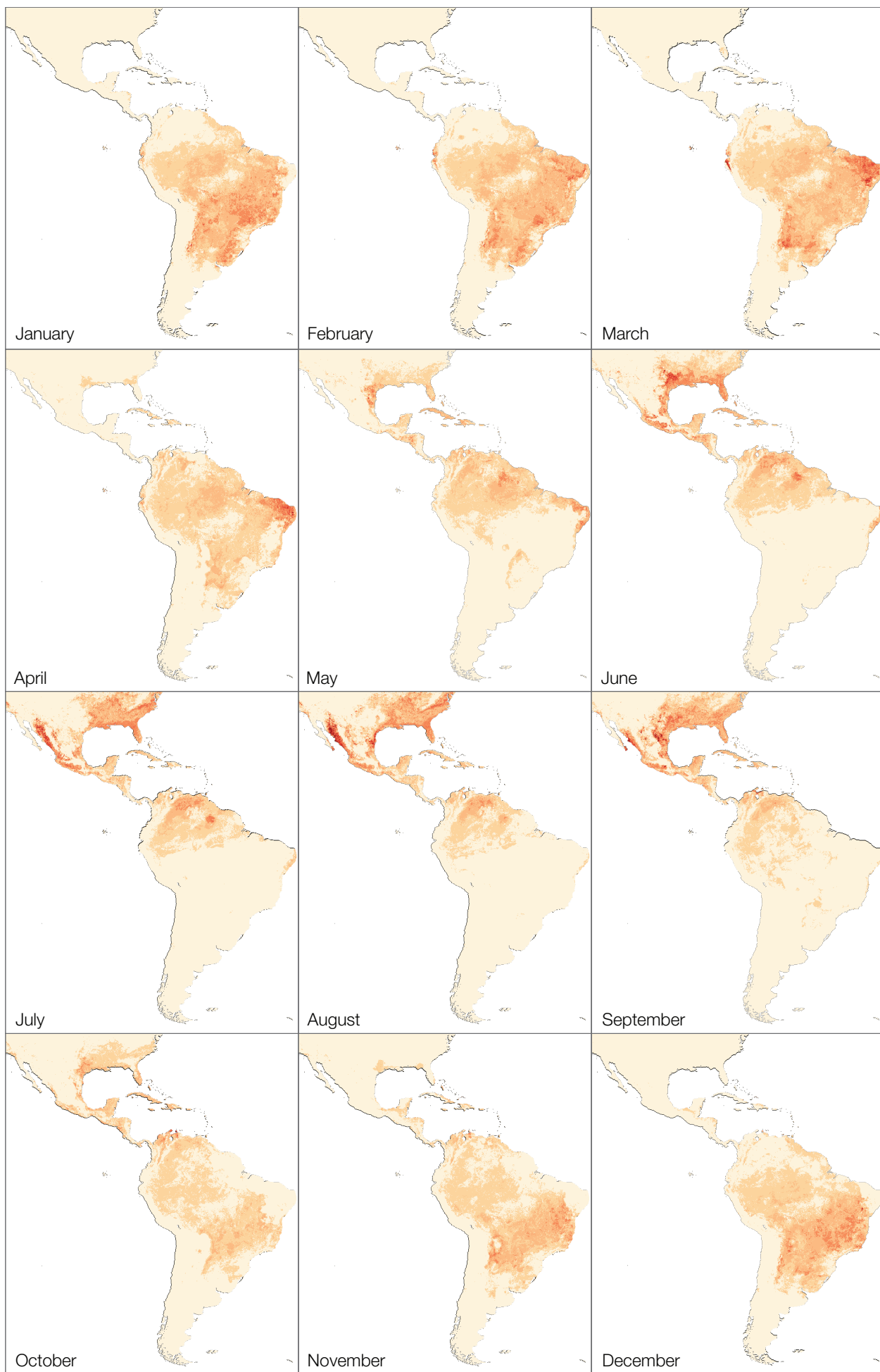
## Ancestral node location posterior probability (DTA)



## Ancestral node location posterior probability (BASTA)

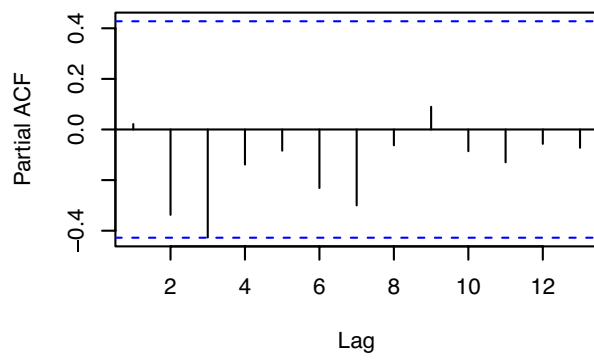




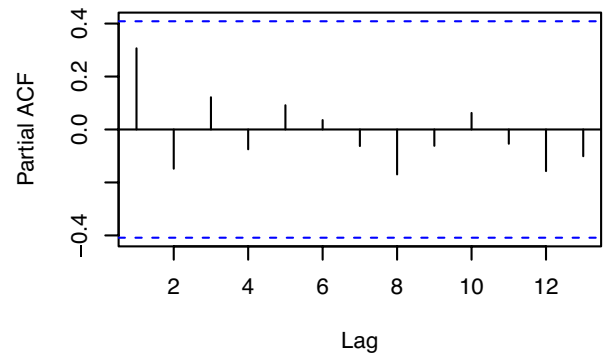




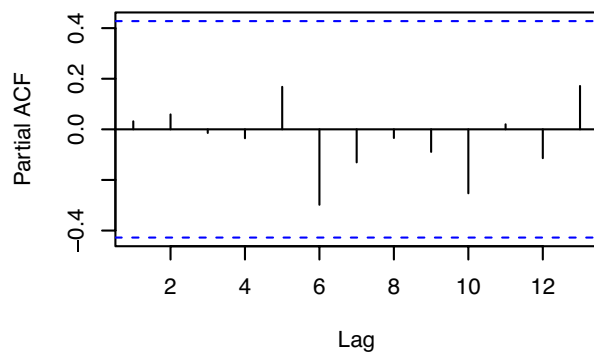
**North**



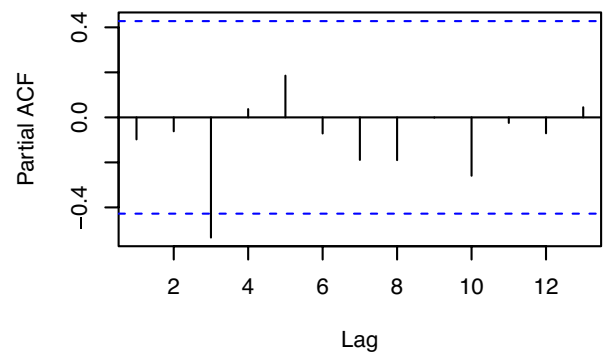
**Northeast**



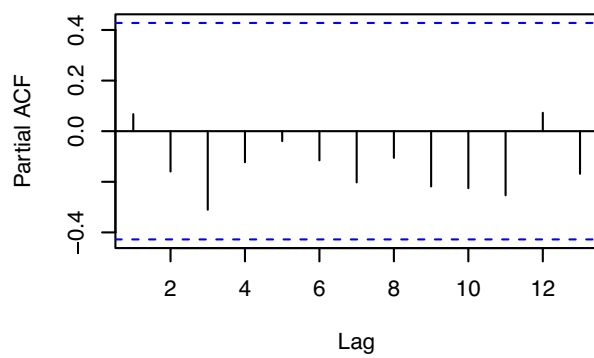
**Centre-West**



**South**



**Southeast**



(a)

Laboratory, Federal state	No. Positives / Tested (%)	Ct value (mean, min- max)	Collection lag (median, min-max)
LACEN, RN	27/335 (8.1%)	35.9 (18.6-39.1)	5 (4-16)
LACEN, PB	26/276 (9.4%)	35.7 (30.7-37.0)	6 (0-88)
FioCruz, PE	95/315 (30%)	34.6 (24.1-38.3)	2.5 (0-33)
LACEN, AL	16/140 (11%)	34.1 (27.1-40.2)	2 (0-3)
FioCruz, BA	17/264 (6.4%)	35.8 (24.7-39.2)	4 (0-228)

(b)

	N	NE	CW	S	SE
Correlated time period	12/2015 to 10/2016	7/2015 to 10/2016	9/2015 to 8/2016	6/2015 to 05/2016	11/2015 to 9/2016
<i>P</i> -value	<0.0001	0.00013	<0.0001	<0.0001	<0.0001
Adjusted- $R^2$	0.929	0.8448	0.987	0.9543	0.953
Time lag (months)	1.27	0	1.12	1.19	1.33

(c)

Region	$R$ (mean, CI), $g=20$ days	$R$ (mean, CI), $g=15$ days	$R$ (mean, CI), $g=10$ days	Growth rate ( $r$ , CI)
CW	1.71 (1.65-1.78)	1.46 (1.20-1.77)	1.29 (1.13-1.46)	0.027 (0.02-0.03)
N	2.48 (2.19-2.81)	1.98 (1.80-2.18)	1.58 (1.48-1.69)	0.046 (0.04-0.05)
NE, 1 <sup>st</sup>	3.12 (2.69-3.60)	2.36 (2.11-2.63)	1.78 (1.65-1.91)	0.06 (0.05-0.07)
NE, 2 <sup>nd</sup>	3.03 (2.74-3.36)	2.31 (2.14-2.49)	1.75 (1.66-1.84)	0.06 (0.05-0.06)
SE	3.85 (3.35-4.42)	2.77 (2.49-3.07)	1.98 (1.84-2.12)	0.07 (0.06-0.076)
S	2.57 (1.72-3.82)	2.04 (1.50-2.75)	1.61 (1.31-1.97)	0.05 (0.04-0.07)

Accession Number	Sample ID	Aligned Reads	Consensus nucleotide bases (% of reference)	RT-qPCR Ct	Collection Date	Municipality	State
KY558989	ZBRA105	58128	9846 (92)	29.5	2015-02-23	João Câmara	RN
KY558990	ZBRC14	19111	8612 (81)	32.81	2016-01-15	Recife	PE
KY558991	ZBRC16	9161	7178 (67)	34.94	2016-01-19	Garanhuns	PE
KY558992	ZBRC18	7183	7459 (70)	35.14	2016-01-06	Caetes	PE
KY558993	ZBRC25	20533	5688 (53)	35.89	2016-01-18	Sanharó	PE
KY558994	ZBRC28	7905	8987 (84)	36.02	2016-01-18	Limoeiro	PE
KY558995	ZBRC301	20826	9843 (92)	31.99	2015-05-13	Paulista	PE
KY558996	ZBRC302	26331	10007 (94)	30.78	2015-05-13	Paulista	PE
KY558997	ZBRC303	12575	5873 (55)	32.81	2015-05-14	Olinda	PE
KY558998	ZBRC313	16530	9478 (89)	30.77	2015-06-15	Paulista	PE
KY558999	ZBRC319	17316	10565 (99)	24.07	2016-07-10	Olinda	PE
KY559000	ZBRC321	11434	8647 (81)	30.62	2015-08-09	Paulista	PE
KY559001	ZBRD103	13192	8380 (78)	29.09	2015-08-20	Murici	AL
KY559002	ZBRD107	77118	7415 (69)	30.31	2015-09-09	Maceió	AL
KY559003	ZBRD116	21211	9785 (92)	27.13	2015-08-28	Arapiraca	AL
KY559004	ZBRE69	2313	6866 (64)	24.72	2016-04-16	Feira de Santana	BA
KY559005	ZBRX1	21267	10559 (99)	25	2016-04-18	Ribeirão Preto	SP
KY559006	ZBRX2	24105	9961 (93)	32	2016-04-18	Ribeirão Preto	SP
KY559007	ZBRX4	14722	10563 (99)	26	2016-04-18	Ribeirão Preto	SP
KY559008	ZBRX6	12516	6893 (64)	33	2016-04-19	Ribeirão Preto	SP
KY559009	ZBRX7	10981	8563 (80)	33	2016-04-19	Ribeirão Preto	SP
KY559010	ZBRX8	7445	8702 (81)	33	2016-04-19	Ribeirão Preto	SP
KY559011	ZBRX11	21214	9379 (88)	31	2016-04-19	Ribeirão Preto	SP
KY559012	ZBRX12	19838	10305 (97)	31	2016-04-19	Ribeirão Preto	SP
KY559013	ZBRX13	11809	10564 (99)	21	2016-04-24	Ribeirão Preto	SP
KY559014	ZBRX14	5873	7469 (70)	33	2016-04-24	Ribeirão Preto	SP
KY559015	ZBRX15	20190	10563 (99)	27	2016-04-24	Ribeirão Preto	SP
KY559016	ZBRX16	9698	9027 (85)	32	2016-04-25	Ribeirão Preto	SP
KY559017	ZBRX100	5976	9609 (90)	28.5	2016-05-19	Ribeirão Preto	SP
KY559018	ZBRX102	13990	9508 (89)	33.91	2016-02-25	Porto Nacional	TO
KY559019	ZBRX103	17635	9514 (89)	36.76	2016-05-24	Araguaina	TO
KY559020	ZBRX106	29877	8458 (79)	32.36	2016-03-07	Palmas	TO
KY559021	ZRBX127	18914	10066 (94)	29.6	2016-03-10	Palmas	TO
KY559022	ZRBX128	18480	8650 (81)	28.79	2016-03-13	Palmas	TO
KY559023	ZBRX130	16667	9914 (93)	29.06	2016-03-22	Palmas	TO
KY559024	ZBRX137	15895	9767 (91)	34.83	2016-03-03	Palmas	TO
KY559025	ZBRY1	41036	8941 (84) †	33.53	2016-01	Rio de Janeiro	RJ
KY559026	ZBRY4	27865	8433 (79) †	34.21	2016-01	Rio de Janeiro	RJ
KY559027	ZBRY6	11779	10300 (97) †	22.66	2016-01	Rio de Janeiro	RJ
KY559028	ZBRY12	4980	3061 (28) †	33.66	2016-01	Rio de Janeiro	RJ
KY559029	ZBRY11	18530	5873 (55) †	31.11	2016-01	Rio de Janeiro	RJ
KY559030	ZBRY10	14067	5712 (53) †	30.84	2016-01	Rio de Janeiro	RJ
KY559031	ZBRY8	5708	9184 (86) †	30.96	2016-01	Rio de Janeiro	RJ
KY559032	ZBRY7	7749	9018 (84) †	28.07	2016-01	Rio de Janeiro	RJ
KY817930	ZBRY14	8040	5389 (50) †	34.2	2016-02-15	Rio de Janeiro	RJ

(a)

Gene	Mean	Lower BCI	Upper BCI
<i>C</i>	0.86	0.65	1.06
<i>prM</i>	0.98	0.85	1.12
<i>E</i>	1.04	0.87	1.24
<i>NS1</i>	0.97	0.83	1.12
<i>NS2A</i>	0.98	0.83	1.13
<i>NS2B</i>	1.12	0.93	1.34
<i>NS3</i>	0.93	0.75	1.11
<i>NS4A</i>	0.87	0.74	1.01
<i>NS4B</i>	1.11	0.9	1.35
<i>NS5</i>	1.35	0.87	1.12

(b)

Clock	Coalescent	PS	SS
UCLN	Skyline	-32090.664	-32116.195
SC	Skyline	-32117.581	-32148.760
UCLN	Exponential	-32193.426	-32218.348
UCLN	Constant	-32206.219	-32234.196
SC	Constant	-32229.262	-32257.900
SC	Exponential	-32244.500	-32270.815

(c)

Clock model	Coalescent prior	Node A TMRCA (95% BCIs)	Node B TMRCA (95% BCIs)	Node C TMRCA (95% BCIs)
SC	Constant	2013.59 (2013.4,2013.77)	2013.83 (2013.6,2014.05)	2013.90 (2013.65,2014.12)
SC	Exponential	2013.59 (2013.38,2013.77)	2013.82 (2013.58,2014.04)	2013.89 (2013.65,2014.11)
SC	Skyline	2013.66 (2013.48,2013.81)	2013.93 (2013.74,2014.14)	2013.99 (2013.75,2014.18)
UCLN	Constant	2013.65 (2013.42,2013.84)	2013.91 (2013.63,2014.2)	2014.04 (2013.73,2014.32)
UCLN	Exponential	2013.66 (2013.45,2013.84)	2013.88 (2013.64,2014.13)	2014 (2013.73,2014.25)
UCLN	Skyline	2013.71 (2013.54,2013.85)	2014.03 (2013.76,2014.26)	2014.16 (2013.89,2014.41)